

ISPE 2024

NOV. 8-10, 2024

INTERNATIONAL SYMPOSIUM

ON PRECISION ENGINEERING

ORGANIZERS



CO-ORGANIZERS



SPONSORS



Table of Contents

Table of Contents	1
Organizers	2
Co-organizers	3
Sponsors	3
General Information	4
The Hotel Formosa, Caotun, Nantou Country Map.....	11
Symposium Agenda	12
Plenary Speakers	13
Keynote Speakers	16
Invited Speakers	18
Oral Sessions	20
Poster Session.....	25
Abstract Collections	30

Organizers



National Chung Hsing University
<http://www.nchu.edu.tw>



National University of Singapore
<https://www.nus.edu.sg>



SCience and Engineering Institute, SCIEI
<http://sciei.org>



Ming Chi University of Technology
<https://www.mcut.edu.tw>

Co-organizers



NCHU GIPE Alumni Association
<http://alumnigipe.nchu.edu.tw>



精密工程
研究所 Graduate Institute
of Precision Engineering

Graduate Institute of Precision Engineering, GIPE
National Chung Hsing University
<https://www.ipe.nchu.edu.tw>



Department of Mechanical Engineering
Ming Chi University of Technology
<https://me.mcut.edu.tw>

Sponsors



Flexible MiCAtronic Industry University Alliance
<https://sites.google.com/view/mica-platform>



Advanced Industry Technology and Precision
Processing Center
National Chung Hsing University
<http://rcaitpp.nchu.edu.tw>

General Information

2024 5th International Symposium on Precision Engineering 2024 (ISPE 2024) will be held at The Hotel Formosa, Caotun, Nantou Country, during November 8 ~ 10, 2024. The main objective of the ISPE 2024 is to provide a major international platform for knowledge exchange and an interactive forum in integrated technologies, mechanical engineering, optics, electronics, electrical engineering and material engineering into precision manufacturing, precision measurement, precision inspection, MEMS, semiconductor and precision environmental control, etc. These are all fascinating topics related to future needs. On behalf of the ISPE 2024 organizing committee, we sincerely welcome you for participating this symposium to share your experience and research results. ISPE 2024 welcomes authors to submit papers on any branch of precision engineering and its applications, and other subjects.

Plenary Speakers

- Chair Prof. Ying-Hao Chu
Associate Vice President for Research and Development
Director of NTHU CNMM
Department of Materials Science and Engineering
National Tsing Hua University, Taiwan
- GlobalFoundries Chair Prof. Chengkuo Lee
Center for Intelligent Sensors and MEMS
Department of Electrical and Computer Engineering
National University of Singapore, Singapore

Keynote Speakers

- Prof. Dr. Chao-Cheng Kaun
Research Center for Applied Sciences, Academia Sinica, Taiwan
- Prof. Uma N. Dulhare
Computer Science & Artificial Intelligence Department
Muffakham Jah College of Engineering & Technology, India

Invited Speakers

- Assoc. Prof. Jyoti Jaiswal
Department of Physics
Rajiv Gandhi University, India
- Assoc. Prof. Ratchatin Chanchaen
Department of Mechanical Engineering
Chulalongkorn University, Thailand
- Assoc. Prof. Teeranoot Chanthasopeephan
Department of Mechanical Engineering
King Mongkut's University of Technology Thonburi, Thailand

Honorary Chair

- President Fuh-Jyh Jan
Department of plant pathology
National Chung Hsing University, Taiwan
- Dean Ming-Der Yang
Department of Civil Engineering
National Chung Hsing University, Taiwan

Symposium Chair

- Prof. Po-Liang Liu
Graduate Institute of Precision Engineering
National Chung Hsing University, Taiwan
- GlobalFoundries Chair Prof. Chengkuo Lee
Department of Electrical and Computer Engineering
National University of Singapore, Singapore

Organizing Chair

- Prof. Vidar Gudmundsson
Science Institute
University of Iceland, Reykjavik, Iceland

Technical Program Chair

- Chair Prof. Yu-Lin Shen
Department of Mechanical Engineering
University of New Mexico, USA

Publication Chair

- Assoc. Prof. Jen-Chuan Tung
Center for General Education
Chang Gung University, Taiwan

Organizing Committee

- Prof. Ming-Chang Lin
Fellow of Academia Sinica, Taiwan
Robert W. Woodruff Professor Emeritus of Emory University, U.S.A.
Center for Emergent Functional Materials Science, Department of Applied
Chemistry, National Yang Ming Chiao Tung University, Hsinchu, Taiwan
- Chair Prof. Charles W. Tu
Department of Electrical Engineering
National Chung Hsing University, Taiwan
- President Dong-Sing Wu
Department of Applied Materials and Optoelectronic Engineering
National Chi Nan University, Taiwan
- Chair Prof. Ray-Hua Horng
Institute of Electronic
National Yang Ming Chiao Tung University, Taiwan
- Dr. Nabila A. Karim
Fuel Cell Institute
Universiti Kebangsaan Malaysia, Malaysia
- Prof. Vidar Gudmundsson
Science Institute
University of Iceland, Iceland
- Ts. Dr. Kean Long Lim
Fuel Cell Institute
Universiti Kebangsaan Malaysia, Malaysia
- Prof. Ngoc Dang Khoa Tran
Faculty of Mechanical Engineering
Industrial University of Ho Chi Minh City, Vietnam
- Chair Prof. Yu-Lin Shen
Department of Mechanical Engineering
University of New Mexico, USA

- GlobalFoundries Chair Prof. Chengkuo Lee
Department of Electrical and Computer Engineering
National University of Singapore, Singapore
- Prof. Bhaskar Kanseri
Department of Physics
Indian Institute of Technology Delhi, New Delhi, India
- Prof. Ho Thanh Huy
Department of Physics and Electronic Engineering
VNU-Ho Chi Minh University of Science, Vietnam
- Prof. Ratchatin Chanchaon
Department of Mechanical Engineering
Chulalongkorn University, Thailand
- Distinguished Prof. Gou-Jen Wang
College of Engineering
National Chung Hsing University, Taiwan
- Distinguished Prof. Hisharng Yang
Graduate Institute of Precision Engineering
National Chung Hsing University, Taiwan
- Distinguished Prof. Pin Han
Graduate Institute of Precision Engineering
National Chung Hsing University, Taiwan
- Distinguished Prof. Dung-An Wang
Graduate Institute of Precision Engineering
National Chung Hsing University, Taiwan
- Prof. Chia-Feng Lin
Department of Materials Engineering
National Chung Hsing University, Taiwan
- Prof. Po-Liang Liu
Graduate Institute of Precision Engineering
National Chung Hsing University, Taiwan

- Distinguished Prof. Ming-Tzer Lin
Graduate Institute of Precision Engineering
National Chung Hsing University, Taiwan
- Prof. and Head Cheng-Mu Tsai
Graduate Institute of Precision Engineering
National Chung Hsing University, Taiwan
- Prof. Congo Tak-Shing Ching
Graduate Institute of Biomedical Engineering
National Chung Hsing University, Taiwan
- Prof. Cheng-Chung Chang
Graduate Institute of Biomedical Engineering
National Chung Hsing University, Taiwan
- Prof. Hui-Min David Wang
Graduate Institute of Biomedical Engineering
National Chung Hsing University, Taiwan
- Assoc. Prof. Fu-Yuan Hsu
Department of Materials Science and Engineering
National United University, Taiwan
- Assoc. Prof. Sheng-Fang Huang
Mechanical Engineering Department
China University of Science and Technology, Taiwan
- Assoc. Prof. Kuo-Chih Liao
Graduate Institute of Biomedical Engineering
National Chung Hsing University, Taiwan
- Assoc. Prof. Shu-Ping Lin
Graduate Institute of Biomedical Engineering
National Chung Hsing University, Taiwan
- Assoc. Prof. Jen-Chuan Tung
Center for General Education
Chang Gung University, Taiwan

- Assoc. Prof. Chih-Liang Wang
Department of Materials Science and Engineering
National Tsing Hua University, Taiwan
- Assoc. Prof. and Head Chian-Hui Lai
Graduate Institute of Biomedical Engineering
National Chung Hsing University, Taiwan
- Assist. Prof. Bill Cheng
Graduate Institute of Biomedical Engineering
National Chung Hsing University, Taiwan
- Assoc. Prof. Zhi-Ting Ye
Department of Mechanical Engineering
National Chung Cheng University, Taiwan
- Assist. Prof. Che-Hao Liao
Department of Electronic Engineering
National Yunlin University of Science and Technology, Taiwan
- Prof. Shih-Hung Lin
Department of Electronic Engineering
National Yunlin University of Science and Technology, Taiwan
- Prof. Chil-Chyuan Kuo
Department of Mechanical Engineering
Ming Chi University of Technology, Taiwan
- Assist. Prof. Chi-Pin Hsu
Department of Mechanical Engineering
Ming Chi University of Technology, Taiwan

Symposium Secretary

Email: nchugipe@gmail.com

Tel: +886-4-2284-0461 Ext.618 (Chinese & English)

Phone: +886-963-841929

The Hotel Formosa, Caotun, Nantou Country Map

Location

Hotel Formosa Located at Bishan road :

- Take 8~10 minute by car from hotel to Freeway No.3 and Jhongtuo Expressway.
- Take 7 minute by car to Chung Hsing New Village.
- Take 15 minute by car to Nantou city and Nangang Industrial District
- Take 50 minute by car to Sun Moon Lake National Scenic Area

By Car

- **【Go south】**
National Highway No.3 → Kuaiguan Interchange towards Caotun Interchange (south) → then exit towards Bo'ai Rd → turn right at Zhongzheng Rd → turn left at Bishan Rd → arrive hotel
- **【Go North】**
National Highway No.3 (224K) → exit at Zhongxing System Interchange and toward Taiwan Provincial Highway 14B → turn right at Shengfu Rd → turn left at Sec. 1, Taiping Rd → turn right at Bishan Rd → arrive hotel

Symposium Agenda

All academic events will be held at The Hotel Formosa, Caotun, Nantou County, Taiwan

Time	Activity		
8 November, 2024 - Only Registration			
15:00~17:00	Registration & Welcome Reception		
9 November, 2024 - Symposium Day			
08:00~08:30	Registration		
08:30~10:00	Invited Talk & Oral Session (1)	Poster Exhibition	
10:00~10:15	Group Photo & Coffee Break		
10:15~10:30	Opening Ceremony		
10:30~11:15	Plenary Speech (1) Ying-Hao Chu		Moderator: Chi-Pin Hsu
11:15~12:00	Keynote Speech (1) Chao-Cheng Kaun		
12:00~13:00	Lunch Time		
13:00~13:45	Plenary Speech (2) Chengkuo Lee		Moderator: Jen-Chuan Tung
13:45~14:30	Keynote Speech (2) Uma N. Dulhare		
14:30~15:45	Invited Talk & Oral Session (2)		
15:00~16:00	Poster Session		
15:45~16:00	Coffee Break		
16:00~17:00	Oral Session (3)		
17:00~18:00	Oral Session (4)		
18:30	Symposium Banquet		
10 November, 2024 - Academic Visit			
09:00~13:30	Academic Visit - JOJOZOO PARK		

Plenary Speaker 1



Chair Prof. Ying-Hao Chu

Associate Vice President for Research and Development

Director of NTHU CNMM

Department of Materials Science and Engineering

National Tsing Hua University, Taiwan

Title of Plenary Speech

Epitaxial Growth of $\text{Bi}_2\text{O}_2\text{X}$ Films and Related Heterostructures

Abstract of Plenary Speech

The pursuit of high-performance electronic devices has driven the research focus towards 2D semiconductors with high electron mobility and suitable bandgap. Previous studies have demonstrated that bismuth oxycompound ($\text{Bi}_2\text{O}_2\text{X}$, X=S, Se, Te, BOX) has remarkable physical properties, such as native oxide layer and ultrahigh carrier mobility, facilitating the development of advanced electronic devices in the sub-silicon era. However, the understanding of the growth of BOX is still unclear, and the methods to control BOX's physical properties should be further explored. Thus, in our lab, the epitaxy of $\text{Bi}_2\text{O}_2\text{Se}$ (BOSe) and $\text{Bi}_2\text{O}_2\text{S}$ (BOS) can be obtained to realize the growth mechanism and secure higher crystallinity. The intrinsic transportation property and photoelectricity of BOX will also be investigated. Furthermore, various control methods have been demonstrated on BOX, including compositional modification, doping process, and non-volatile modulation. With these efforts, the controlled methods provide pathways to manipulate the electrical properties of BOX and corresponding devices, further advancing this material system for development in the next-generational electronics.

Plenary Speaker 2



GlobalFoundries Chair Prof. Chengkuo Lee

*Center for Intelligent Sensors and MEMS
Department of Electrical and Computer Engineering
National University of Singapore, Singapore*

Title of Plenary Speech

CMOS Photonics – Extending Si Photonics to In-Sensor Computing and Nanophotonic Sensing Platforms

Abstract of Plenary Speech

In the rapidly evolving field of artificial intelligence of things (AIoT), a key challenge is to process sensing signals efficiently while minimizing latency and power consumption. Traditional microelectronic systems face limitations in speed and energy efficiency, prompting the exploration of photonic integrated circuits for their superior data transmission and computational capabilities. Silicon Photonic integrated Circuits (Si PIC) offer miniaturized solutions for multimodal spectroscopic sensory systems by leveraging the simultaneous interaction of light with temperature, chemicals, and biomolecules. Furthermore, Si and AlN waveguides can manipulate light-matter interactions at the nanoscale, become an appealing CMOS Photonics platform for photonics neural networks (PNN) computation application and diversified biochemical and physical sensing applications with high sensitivity and small footprints. The multimodal spectroscopic sensory data is complex and shows huge data volume with high redundancy, thus requiring high communication bandwidth associated with high communication power consumption to transfer the sensory data. To circumvent this high communication cost, we bring the photonic sensor and processor into intimacy and propose a photonic multimodal in-sensor computing system using an integrated silicon photonic convolutional processor.

On the other hand, surface plasmons have proven their ability to boost the sensitivity of mid-infrared hyperspectral imaging by enhancing light-matter interactions. Recently, we have investigated the phonons in hyperspectral bioimaging by developing a synergistic plasmon-phonon system. We demonstrated that phonons, in synergy with plasmons, enhance the per-second spectral de-overlapping functionality in imaging dynamic reaction process involved with COVID viruses.

Keynote Speaker 1



Prof. Dr. Chao-Cheng Kaun

Research Center for Applied Sciences, Academia Sinica, Taiwan

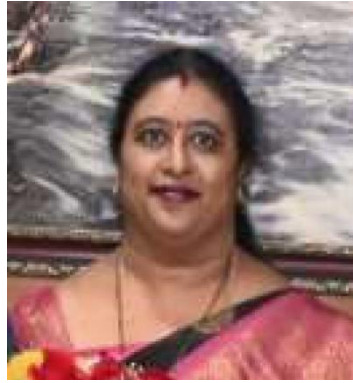
Title of Keynote Speech

Driving noncollinear interlayer exchange coupling intrinsically in magnetic trilayers

Abstract of Keynote Speech

Ferromagnetic side layers sandwiching a nonmagnetic spacer as a metallic trilayer has become a pivotal platform for achieving spintronic devices. Recent experiments demonstrate that manipulating the width or the nature of conducting spacer induces noncollinear magnetic alignment between the side layers. Our theoretical analysis reveals that altering the width of spacer significantly affects the interlayer exchange coupling (IEC), resulting in noncollinear alignment. Through analytic and first-principles methods, our study on the Fe/Ag/Fe trilayer shows that at a specific width of the Ag spacer, the magnetic moments of side layers tend to be perpendicular. This alignment is mediated by Ag quantum well states, exhibiting spin spirals across the trilayer. Our results reveal that the noncollinear IEC offers a degree of freedom to control magnetic devices and boost spintronic technology with improved transport capabilities.

Keynote Speaker 2



Prof. Uma N. Dulhare

*Computer Science & Artificial Intelligence Department,
Muffakham Jah College of Engineering & Technology, India*

Title of Keynote Speech

Harnessing Deep Learning for Precision Diagnostics in Dermatology and Rheumatology

Abstract of Keynote Speech

Deep learning is becoming essential in revolutionizing medical diagnostics and personalized care for skin lesions and rheumatoid arthritis. As a subset of AI becomes more integrated into healthcare, it significantly improves diagnostic accuracy, treatment optimization and research advancement in dermatology and rheumatology.

A proposed framework leveraging convolutional neural networks (CNNs) with hybrid architecture is designed to detect and classify various skin lesions including melanoma and nodules with enhanced precision, early intervention and better prognosis. Furthermore, deep learning is providing new insights into rheumatoid nodules by integrating multimodal data such as imaging and patient histories, leading to a better understanding of nodule progression and personalized treatment for autoimmune conditions like rheumatoid arthritis (RA).

Experimental studies shows a pathway of relationship between skin lesions and rheumatoid arthritis progression. These finding shed light on how inflammation can contribute to secondary skin conditions, recommending disease management and treatment strategies.

Invited Speaker 1



Assoc. Prof. Jyoti Jaiswal

*Department of Physics, Rajiv Gandhi University
Rono-Hills, Doimukh, Arunachal Pradesh, India*

Title of Invited Talk

Novel miniaturized pH sensing technologies for advanced health and biomedical applications

Abstract of Invited Talk

The discovery of miniaturized pH sensing technologies represents an important frontier in modern health care and biomedical research. These miniature sensors promise to revolutionize diagnosis, treatment monitoring, and disease management by providing real-time, non-invasive, and accurate measurement of pH levels in various biological environments. From microneedle pH sensors to microfluidic pH sensors and flexible e-skin pH sensors, the spectrum of miniaturized pH sensing technologies offer a diverse range of devices designed for advanced health and biomedical applications. However, the development of these miniature pH sensing technologies is not without its challenges. Some hurdles include achieving high sensitivity and accuracy while maintaining the miniaturized dimensions required for seamless integration into biological systems and the design and fabrication of miniature sensors capable of withstanding the complex and dynamic conditions within the human body. Moreover, ensuring biocompatibility, long-term stability, and ease of use are critical considerations that must be addressed to unlock the full potential of these technologies in biomedical applications. In this context, we have probed into the design and development of various miniature pH sensing technologies, exploring the challenges encountered along the way and invented innovative solutions to overcome them. Recently, we reported, for the first time, a new design of miniaturized microneedle pH sensors based on $\text{AgIO}_3/\text{Ag}/\text{PTFE}/\text{WO}_3/\text{W}$, enabling in-situ real-time pH monitoring of small biological entities, such as fish eggs. Additionally, we recently proposed a novel microfluidic pH sensor using $\text{Sb}_2\text{O}_3/\text{Sb}$ and

AgIO₃/Ag thin films, demonstrating robust Nernstian sensitivity, linear correlation coefficient, stability over time, and in-vitro pH testing of human lung cancer (A549) cells with minimal sample volumes. We also recently introduced a novel flexible on-skin wearable pH sensor patch composed of PDMS, incorporating thin films of Sb₂O₃/Sb and AgIO₃/Ag for real-time sweat sensing to monitor pH levels across various body parts, which is highly desirable for sports medication and personal wellness. Overall, this talk would present new results in the design and development of various miniature pH sensing technologies for advanced health and biomedical applications.

Invited Speaker 2



Associate Professor Dr. Ratchatin Chancharoen

*Department of Mechanical Engineering, Robotics and AI Program
Chulalongkorn University, Thailand*

Title of Invited Talk

Collaborative 3D Welding Robots with Augmented Vision Utilizing the Digital Twin Concept

Abstract of Invited Talk

This project, in collaboration with industry, focuses on enhancing the precision of collaborative 3D welding robots through the integration of digital twins and sensor fusion. A key challenge lies in managing the 3D trajectory, where errors in both position and time must be carefully addressed to ensure accurate weld joint alignment and execution. The task becomes even more complex due to the use of a heavy welding tool and the nature of the part being welded, which is not rigid or uniform, adding further variability to the process. Additionally, limitations in measurement accuracy, caused by sensor constraints and the difficulty of capturing real-time data in dynamic environments, present further obstacles. To address these issues, extensive mapping techniques are utilized to model and adjust for spatial and temporal discrepancies, while advanced image processing algorithms are applied to analyze and correct weld joint deviations. These strategies are crucial for compensating for trajectory errors and achieving the required precision despite the significant challenges inherent to the system.

Invited Speaker 3



Associate Professor Dr. Teeranoot Chanthasopeephan

Department of Mechanical Engineering

King Mongkut's University of Technology Thonburi, Bangkok, Thailand

Title of Invited Talk

Hybrid PI-Neural Network Control of a Fluid-Driven Origami-Inspired Pneumatic Artificial Muscle

Abstract of Invited Talk

This research focuses on the development and design of a lower limb exoskeleton inspired by pneumatic artificial muscles (PAMs). PAMs are highly valued as actuators due to their low weight, favorable mass-to-force ratio, compliance, and ability to closely mimic the function of human biological muscles. These characteristics make them well-suited for applications in robotics and rehabilitation. However, PAMs pose significant challenges in modeling and control, given their time-varying parameters, complex hysteresis behavior, and nonlinear dynamics.

To address these challenges, we propose a novel approach for controlling PAM-driven systems, specifically focusing on a fluid-driven origami-inspired artificial muscle (FOAM). The control strategy utilizes a hybrid control algorithm that integrates a proportional-integral (PI) controller with a feed-forward neural network. This combination allows the controller to adapt and learn from the system's behavior, improving its responsiveness and accuracy over time.

The proposed control algorithm was tested for its ability to manage displacement control in FOAM under varying input signals. Additionally, experiments were conducted to assess the controller's performance under different load conditions. The results demonstrate that the control system exhibits excellent adaptability and robustness. These findings highlight the potential of this hybrid approach for enhancing PAM-based systems in dynamic environments, making them highly suitable for rehabilitation and robotic applications.

Oral Sessions

Nov. 9, 2024

Session 1

Precision manufacturing machines and technologies

Session Chair: Assist. Prof. Chi-Pin Hsu

Department of Mechanical Engineering

Ming Chi University of Technology

08:30~10:00	I-1	<p>Novel miniaturized pH sensing technologies for advanced health and biomedical applications</p> <p><i>Jyoti Jaiswal</i>[†]</p> <p>Department of Physics, Rajiv Gandhi University, India</p>
	I-2	<p>Collaborative 3D Welding Robots with Augmented Vision Utilizing the Digital Twin Concept</p> <p><i>Ratchatin Chanchaoen</i>[†]</p> <p>Mechanical Engineering Department, Robotics and AI Program, Chulalongkorn University, Thailand</p>
	O-2	<p>Mannose-modified Interfaces in the Application of Anti-cancer Drug Loading or Bio-Sensing</p> <p><i>Chian-Hui Lai</i>^{†,*}</p> <p>Graduate Institute of Biomedical Engineering National Chung Hsing University, Taiwan</p>
	O-9	<p>PVDF-Muscovite bimorph system as flexible transparent thermal sensor</p> <p><i>Ching-Ming Su</i>^{†,1}, <i>Jyh-Ming Wu</i>², <i>Che-Ning Yeh</i>², and <i>Ying-Hao Chu</i>^{2,*}</p> <p>¹ Department of Materials Science and Engineering, National Yang Ming Chiao Tung University, Taiwan ² Department of Materials Science and Engineering, National TsingHua University, Taiwan</p>

	O-7	<p>Interfacial Characteristics on the Joint of unidirectional Carbon fiber reinforced thermoplastics Composite /Aluminum alloy laminate</p> <p><i>Ming-Yuan Shen</i>*, <i>Chih-Hsien Cheng</i>†, and <i>Shin-Yu Chen</i></p> <p>Department of Mechanical Engineering, National Chin-Yi University of Technology, Taiwan</p>
08:30~10:00	O-1	<p>A simplified method for joining polyetheretherketone and aluminum 6061 dissimilar materials based on the interface structure of aluminum rods</p> <p><i>Chil-Chyuan Kuo</i>*^{1,2}, <i>Armaan Farooqui</i>†¹</p> <p>¹ Department of Mechanical Engineering, Ming Chi University of Technology ² Research Center for Intelligent Medical Devices, Ming Chi University of Technology</p>

Session 2

Optics, Photonic and Optomechatronic Engineering

Session Chair: Assoc. Prof. Zhi-Ting Ye

Co-Chair: Assoc. Prof. Chia-Hsien Teng

Graduate Institute of Opto-Mechatronics, Department of Mechanical Engineering

National Chung Cheng University

14:30~15:35	I-3	Hybrid PI-Neural Network Control of a Fluid-Driven Origami-Inspired Pneumatic Artificial Muscle <i>Teeranoot Chanthasopeephan[†]</i> Mechanical Engineering Department King Mongkut's University of Technology Thonburi, Thailand
	O-3	Microstructure and Microwave Dielectric Properties of Low-Temperature Sintering $Mg_{2-x}Mn_xV_2O_7$ Ceramic for 5G communication components <i>Zhong-Hao Wang^{†,1}, Yong-Tai Xu¹, Che-Hao Liao¹, Chia-Hung Chang², and Shih-Hung Lin^{*,1}</i> ¹ Department of Electronic Engineering National Yunlin University of Science and Technology, Taiwan ² Department of Electrical Engineering National Yunlin University of Science and Technology, Taiwan
	O-4	Microwave dielectric properties of $CaTi_{1-x}(Co_{1/3}Nb_{2/3})_xO_3$ for applications in high-frequency device <i>Yu-Hsuan Tseng^{†,1}, Jyun-Fong Lin¹, Che-Hao Liao¹, Chia-Hung Chang², and Shih-Hung Lin^{*,1}</i> ¹ Department of Electronic Engineering National Yunlin University of Science and Technology, Taiwan ² Department of Electrical Engineering National Yunlin University of Science and Technology, Taiwan
	O-11	Optimization of Telecentric Lens Design Using Zemax for Precision Machine Vision <i>Ming-Ren Liu^{†,*} and Cheng-Mu Tsai</i> Graduate Institute of Precision Engineering, National Chung Hsing University, Taiwan

14:30~15:35	O-14	<p>Silicon Photonics Switch with Electrostatic MEMS Actuator and Zero Power Consumption in Steady State</p> <p><i>Jyun-Yan Luo[†], Wei-Siang Dai, Jin-Jia Ye, Chen-Yu Fu, and Chun-Wei Tsai*</i></p> <p>Department of Electronic Engineering, National United University, Taiwan</p>
-------------	------	---------------------------------------------------------------------------------------------------------------------------------------------------------------------------------------------------------------------------------------------------------------------------------------------------

Session 3

Micro Manufacturing and Optomechatronic Engineering

Session Chair: Assoc. Prof. Chun-Wei Tsai

Moderator: Assist. Prof. Jen-Chuan Tung

Department of Electronic Engineering

National United University, Taiwan

16:00~17:00	O-10	<p>Research on U-Net thyroid nodule segmentation based on attention mechanism</p> <p><i>Shi-Hong Qiu^{†,*1}, Cheng-Mu Tsai¹, and Chuan-Wang Chang²</i></p> <p>¹ Graduate Institute of Precision Engineering, National Chung Hsing University, Taiwan ² Department of Computer Science and Information Engineering, National Chin-Yi University of Technology, Taiwan</p>
	O-13	<p>LEDs Application of Virtual Factory Environment Simulation in Safety Education Training</p> <p><i>Chiao-Ling Lin^{†,1}, Shih-Hung Lin², and Yao-Chin Wang^{*,1}</i></p> <p>¹ Department of Computer Science and Information Engineering Cheng Shiu University, Taiwan ² Department of Electronic Engineering, National Yulin University of Science and Technology, Taiwan</p>
	O-8	<p>AlN SAW Humidity Sensing Enhancement with SiO₂ Nanoparticles</p> <p><i>Lu-Xiang Wang[†], Zhong-Hong Yen, Che-Hao Liao, Shih-Hung Lin, and Chien-Sheng Huang[*]</i></p> <p>Department of Electronic Engineering National Yunlin University of Science and Technology, Taiwan</p>
	O-5	<p>UV detector fabricated using ZnO thin film prepared by RF magnetron sputtering with a raw powder target</p> <p><i>Wei-Cheng Pan[†], Lin-Yi Tang, Che-Hao Liao, and Chien-Sheng Huang[*]</i></p> <p>Department of Electronic Engineering National Yunlin University of Science and Technology, Taiwan</p>

Session 4

Electronic, Photonic and Optomechatronic Engineering

Session Chair: Assoc. Prof. Che-Hao Liao

Moderator: Assist. Prof. Jen-Chuan Tung

Department of Electronic Engineering

National Yunlin University of Science and Technology, Taiwan

17:00~18:00	O-6	Enhancing Field of View in 3D Floating Holographic Display Using Multiple LCoS-SLMs <i>Hao-Ming Kuo[†], Jun-Yan Luo, Cang-Ci Guo, and Chun-Wei Tsai[*]</i> Department of Electronic Engineering, National United University, Taiwan
	O-15	A Mach-Zehnder Modulator with One-Dimensional Photonic Crystal Filter and Integrated Liquid Crystal Material <i>Cang-Ci Guo[†], Hao-Ming Kuo, Yu-Sheng Kan, Zhi-Xiang Huang, and Chun-Wei Tsai[*]</i> Department of Electronic Engineering, National United University, Taiwan
	O-12	Design of Silicone Light Guide with Mini LED in Automotive Headlamps <i>Yu Fu Hsu[†], Chia Chun Hu, Yang Jun Zheng, and Zhi Ting Ye[*]</i> Graduate Institute of Opto-Mechatronics, Department of Mechanical Engineering, National Chung Cheng University, Taiwan
	O-16	Performance Analysis and Optimization of Ship and Human Recognition in 2D Optical Radar Images Based on YOLOv7 <i>Li-Lin Chen^{†,*} and Yao-Chin Wang</i> Department of Computer Science and Information Engineering Cheng Shiu University, Taiwan

Poster Session

Poster No.	Paper Title
P-1	<p>Enhancing the bending strength of polylactic acid biomedical polymer rods using ultrasound-assisted continuous drive friction welding</p> <p><i>Chil-Chyuan Kuo^{*,1,2} and Hong-Wei Chen^{†,3}</i></p> <p>¹ Department of Mechanical Engineering, Ming Chi University of Technology ² Research Center for Intelligent Medical Devices, Ming Chi University of Technology ³ International Ph. D. Program in Innovative Technology of Biomedical Engineering and Medical Device, Ming Chi University of Technology</p>
P-2	<p><i>Ab initio</i> Studies of Work Function Changes of NO Adsorption on ZnGa₂O₄(111) Surface for Gas Sensors</p> <p><i>Jhih-Hong Shao¹, Guan-Yu Chen^{†,1}, and Po-Liang Liu^{*,1,2}</i></p> <p>¹ Graduate Institute of Precision Engineering, National Chung Hsing University, Taiwan ² Department of Applied Materials and Optoelectronic Engineering, National Chi Nan University, Taiwan</p>
P-3	<p>Highly Sensitive Anti-Resonance Liquid Core Fiber Fabry-Perot Interferometer</p> <p><i>Han-Wei Xie[†], Bing-Qiu Lai, and Cheng-Ling Lee[*]</i></p> <p>Department of Electro-Optical Engineering, National United University, Taiwan</p>
P-4	<p>Designs of a Badminton Training Assistant System with Recognition of Badminton Stroke Gestures by a Deep Learning Strategy of Dual-Modality Sensor Data of Both Imaging RGB and Wearable IMU</p> <p><i>Ing-Jr Ding^{†,*}, Cheng-Feng Yang, Cheng-Yan Hu, and Bing-Cheng Gan</i></p> <p>Department of Electronic Engineering, National United University, Taiwan</p>

P-5	<p>Reconstruction of Multimode Optical Fiber Transmission Images Using Pix2Pix GAN</p> <p><i>Jin-Lin Wang^{†,1}, Hsu-Chih Cheng^{*,1}, and Chun-Ming Huang²</i></p> <p>¹ Department of Electro-Optical Engineering, National Formosa University, Taiwan ² Department of Electronic Engineering, National Formosa University, Taiwan</p>
P-6	<p><i>Ab initio</i> Studies of Work Function Changes of NO Combined with NO₂, CO, CO₂, H₂S, and O₃ Co-Adsorption on ZnGa₂O₄(111) Surface for Gas Sensors</p> <p><i>Guan-Yu Chen^{†,1} and Po-Liang Liu^{*,1,2}</i></p> <p>¹ Graduate Institute of Precision Engineering, National Chung Hsing University, Taiwan ² Department of Applied Materials and Optoelectronic Engineering, National Chi Nan University, Taiwan</p>
P-7	<p>Enhanced Performance of MOCVD grown Zn-doped β-Ga₂O₃ Deep-Ultraviolet Photodetectors on Si Substrates via TiN Buffer Layers</p> <p><i>Tung-Han Wu[†], Wen-Hao Li², Anoop Kumar Singh^{2,3}, Jun-Hong Shen¹, Shiming Huang^{2,3}, Wei-Hsiang Chiang², Hsin-Yu Chou², Po-Liang Liu^{#,1,3}, Ray-Hua Horng⁴, and Dong-Sing Wu^{*,2,3}</i></p> <p>¹ Graduate Institute of Precision Engineering, National Chung Hsing University, Taiwan ² Department of Materials Science and Engineering, National Chung Hsing University, Taiwan ³ Department of Applied Materials and Optoelectronic Engineering, National Chi Nan University, Taiwan ⁴ Institute of Electronics, National Yang Ming Chiao Tung University, Taiwan</p>
P-8	<p>Effects of progressive energy and single energy on the electrical performance of Ar ion-implantation AlGaInP Micro-LEDs</p> <p><i>Shiang-Jiun Lo^{†,1}, Yu-Chih Hsu¹, Yen-Ru Chen¹, Wei-Hsiang Chiang², Po-Liang Liu^{*,1,3}, and Dong-Sing Wu^{*,2,3}</i></p> <p>¹ Graduate Institute of Precision Engineering, National Chung Hsing University, Taiwan ² Department of Materials Science and Engineering, National Chung Hsing University, Taiwan ³ Department of Applied Materials and Optoelectronic Engineering, National Chi Nan University, Taiwan</p>

P-9	<p>Investigation of Smart Fan</p> <p><i>Hsinn-Jyh Tzeng^{†,*} and jia-hao Huang</i></p> <p>Department of Mechanical Engineering, Southern Taiwan University of Science and Technology, Taiwan</p>
P-10	<p>Application of MnCsPb(Br_{0.4}/I_{0.6})₃ perovskite quantum dots in sensitized solar cells</p> <p><i>Feng-Yuan Hsu^{†,1}, Min-Han Chiang¹, Wei-Hsiang Chiang¹, Hsin-Yu Chou¹, and Dong-Sing Wu^{*,1,2}</i></p> <p>¹ Department of Materials Science and Engineering, National Chung Hsing University, Taiwan ² Department of Applied Materials and Optoelectronic Engineering, National Chi Nan University, Taiwan</p>
P-11	<p><i>Ab-initio</i> Study of Bi₂O₂X(X = Se, S, and Te)(001)/SrTiO₃(001) Heterostructures</p> <p><i>Yan-Cheng Lin¹, Chun-Che Lee^{†,1} and Po-Liang Liu^{*,1,2}</i></p> <p>¹ Graduate Institute of Precision Engineering, National Chung Hsing University, Taiwan ² Department of Applied Materials and Optoelectronic Engineering, National Chi Nan University, Taiwan</p>
P-12	<p>Flexible High Entropy Relaxor with Ultrahigh Energy Performance and Outstanding Piezo-respond</p> <p><i>Yu-En Pan^{†,1} and Ying-Hao Chu^{*,2}</i></p> <p>¹ College of Semiconductor Research, National Tsing Hua University, Taiwan ² Department of Materials Science and Engineering, National Tsing Hua University, Taiwan</p>
P-13	<p>Single-Crystalline Ag Nanocrystals Intercalated Muscovite</p> <p><i>Chia-Yun Song^{†,1}, Wan-Zhen Hsieh², Ching-Yu Chiang², Kuo-Ping Chen³, and Ying-Hao Chu^{*,4}</i></p> <p>¹ Department of Materials Science and Engineering, National Yang Ming Chiao Tung University, Taiwan ² National Synchrotron Radiation Research Center, Taiwan ³ Institute of Photonics Technologies, Department of Electrical Engineering, National Tsing Hua University, Taiwan ⁴ Department of Materials Science and Engineering, National Tsing Hua University, Taiwan</p>

P-14	<p>Flexible Magnetoelectric Transducer Based on Muscovite Heterostructure</p> <p><i>Ya-Jing Wu[†], Yong-Jyun Wang, and Ying-Hao Chu[*]</i></p> <p>Department of Materials Science and Engineering, National Tsing Hua University, Taiwan</p>
P-15	<p>Investigating the stability of microwave synthesized Pt-free catalysts for anion exchange membrane fuel cells</p> <p><i>Yi-Jun Chen^{†,1}, Li-Hsiang Lu¹, Chih-Liang Wang^{*,1,2}, and Hsiharnng Yang¹</i></p> <p>¹ Graduate Institute of Precision Engineering, National Chung Hsing University, Taiwan ² Department of Materials Science and Engineering, National Tsing Hua University, Taiwan</p>
P-16	<p>DESIGN AND COMPARISON OF ACCELERATION FEEDBACK CONTROL FOR IMPROVING THE VIBRATION SUPPRESSION AND MOTION PERFORMANCE OF SERVOMECHANISMS</p> <p><i>Yu-Min Ren^{†,1} and Syh-Shiuh Yeh^{*,2}</i></p> <p>¹ Institute of Pioneer Semiconductor Innovation, National Yang Ming Chiao Tung University, Taiwan ² Institute of Electronics, National Yang Ming Chiao Tung University, Taiwan</p>
P-17	<p>First Principles Study of Band Structures with Vertical Electric Field of Bi₂O₂S and Bi₂O₂Te Structures</p> <p><i>Tzu-Wei Wang^{†,1}, Sylvia Qingyu Cai², Chao-Cheng Kaun², and Po Liang Liu^{*,1,3}</i></p> <p>¹ Graduate Institute of Precision Engineering, National Chung Hsing University, Taiwan ² Research Center for Applied Sciences, Academia Sinica, Taiwan ³ Department of Applied Materials and Optoelectronic Engineering National Chi Nan University, Taiwan</p>
P-18	<p>Integrated Microfluidic Photoresistor System for Determining Human Serum Albumin</p> <p><i>To-Lin Chen[†], Kuan-Hsun Huang, Ching-Ti Wang, and Lung-Ming Fu[*]</i></p> <p>Department of Engineering Science, National Cheng Kung University, Taiwan</p>

P-19	<p>Development of a Rapid Microfluidic System for Detecting Magnesium Ion in Serum</p> <p><i>Hsing-Meng Wang¹, Cheng-Xue Yu^{†,2}, Ching-Ti Wang², and Lung-Ming Fu^{*,2}</i></p> <p>¹ Department of Biomechatronics Engineering, National Pingtung University of Science and Technology, Taiwan ² Department of Engineering Science, National Cheng Kung University, Taiwan</p>
P-20	<p>Research of FeCoN-MgOAc/XC-72R as cathode catalysts in Alkaline Anion Exchange Membrane Fuel Cells</p> <p><i>Ting-Syuan Li, Chia-Hsien Ko[†], and Hsiharnng Yang[*]</i></p> <p>Graduate Institute of Precision Engineering, National Chung Hsing University, Taiwan</p>
P-21	<p>NiCoFe layered hydroxide anode catalyst for hydrogen production in anion exchange membrane water electrolysis</p> <p><i>Wei-Ming Chen, Ko-Hsiang Huang[†], and Hsiharnng Yang[*]</i></p> <p>Graduate Institute of Precision Engineering, National Chung Hsing University, Taiwan</p>
P-22	<p>Highly Stable ITO-based Heater With Interdigitated Electrodes</p> <p><i>Nan-Ming Lin^{†,*1}, Shih-Chang Shei², Zhi-Hong Yu², and Shu-Wen Yang³</i></p> <p>¹ Stanch Stainless Steel Co. Ltd, Taiwan ² Department of Electrical Engineering, National University of Tainan, Taiwan ³ Plan Management Section, Metal Industries Research & Development Centre, Taiwan</p>
P-23	<p>Electrodes Electronic, and magnetic properties of the 3d transition metals substitution positions in ZnX₂O₄ (X=Al, Ga) spinel oxide: a GGA+U study</p> <p><i>Jen-Chuan Tung^{†,1} and Po Liang Liu^{*,2,3}</i></p> <p>¹ Center for General Education, Chang Gung University, Taiwan ² Graduate Institute of Precision Engineering, National Chung Hsing University, Taiwan ³ Department of Applied Materials and Optoelectronic Engineering National Chi Nan University, Taiwan</p>

Abstract Collections

No. O-1

TITLE: A simplified method for joining polyetheretherketone and aluminum 6061 dissimilar materials based on the interface structure of aluminum rods

Chil-Chyuan Kuo^{*,1,2} and Armaan Farooqui^{†,1}

¹ Department of Mechanical Engineering, Ming Chi University of Technology

² Research Center for Intelligent Medical Devices, Ming Chi University of Technology

[†]Presenter

*Corresponding author's e-mail: jacksonk@mail.mcut.edu.tw

ABSTRACT

The study uses rotary friction welding to investigate a novel method for joining polyetheretherketone (PEEK) and aluminum 6061 dissimilar materials. The research focuses on optimizing the interface geometry by employing both bored and dovetail designs, which aim to enhance joint strength and durability. The aluminum interface is preheated using a laser welding machine before performing rotary friction welding with PEEK to improve the welding process. This approach is designed to achieve a more robust and reliable bond, particularly by ensuring a stronger interface through controlled preheating. The experimental results demonstrate that the modified interface designs, coupled with preheating, significantly enhance the mechanical properties of the welded joints. The findings provide valuable insights into the development of advanced joining techniques for dissimilar materials, contributing to the broader application of PEEK and aluminum composites in various industries. The proposed method shows promise in reducing material wastage and energy consumption, aligning with sustainable manufacturing practices. Future work will explore the long-term durability of these joints under various operational conditions.

Keyword: Polyetheretherketone; Aluminum 6061; Rotary friction welding; Interface design; Preheating; Laser welding; Dissimilar materials

REFERENCES

- [1] A. A. Lassila, D. Lönn, T. Andersson, W. Wang, and R. Ghasemi, "Effects of different laser welding parameters on the joint quality for dissimilar material joints for battery applications," *Optics & Laser Technology*, vol. 177, p. 111155, **2024**.
- [2] Y. Huang, X. Meng, Y. Wang, Y. Xie, and L. Zhou, "Joining of aluminum alloy and polymer via friction stir lap welding," *Journal of Materials Processing Technology*, vol. 257, pp. 148-154, **2018**.
- [3] K. Schrickler, L. Samfaß, M. Grätzel, G. Ecke, and J. P. Bergmann, "Bonding mechanisms in laser-assisted joining of metal-polymer composites," *Journal of Advanced Joining Processes*, vol. 1, p. 100008, **2020**.
- [4] J. Qi, Y. Bao, J. Wang, L. Li, and W. Li, "Flexural behavior of an innovative dovetail UHPC joint in composite bridges under negative bending moment," *Engineering Structures*, vol. 200, p. 109716, **2019**.
- [5] K. Bula, T. Sterzyński, M. Piasecka, and L. Róžański, "Deformation mechanism in mechanically coupled polymer-metal hybrid joints," *Materials*, vol. 13, no. 11, p. 2512, **2020**.

No. O-2

TITLE: Mannose-modified Interfaces in the Application of Anti-cancer Drug Loading or Bio-Sensing

Chian-Hui Lai^{†,*}

Graduate Institute of Biomedical Engineering, National Chung Hsing University, Taichung 402, Taiwan

[†]Presenter

*Corresponding author's e-mail: chianhuilai@dargon.nchu.edu.tw

ABSTRACT

Our lab work is addressed on the molecular-level design to fabricate an anticancer drug carrier or bio-sensing platform. For the bio-sensing, a label-free and ultrasensitive electrochemical impedance cyto-sensor was developed to specifically detect the MDA-MB-231 cells, a triple-negative breast cancer cell, via the interaction between the mannosyl glassy carbon electrode (GCE) and the overexpressed mannose receptors on the target cell surface.[1] A recycle-used GCE surface based on host-guest interaction was further developed for fungicide detection.[2] For the drug delivery, silica-based Man@Cy3SiO₂NPs were developed, which has great potential for cell image.[3] The data showed that the best specific cellular uptake rate of Man@Cy3SiO₂NPs size is about 250 nm.[2] M-mDOX@SiO₂ was then designed to target cancer cells and release the DOX in an acidic tumor microenvironment (TME).[4] The polymeric nanoparticles (BDOX-GOx@NPs) were further prepared where the polymers were synthesized by the combination of reversible addition–fragmentation chain transfer (RAFT) polymerization method and Cu(I)-catalyzed azide–alkyne cycloaddition click chemistry. BDOX-GOx@NPs equip targeting properties to cancer cells, poly(ethylene glycol) (PEG) for biocompatibility, and aryl-aldehyde moieties for enzyme glucose oxidase (GOx) immobilization. The bioactivity of the BDOX-GOx@NPs nanoplatform in the two- and three-dimensional models of MDA-MB-231 cancer cells was investigated to ascertain its antitumor efficacy.[5]

Keyword: MDA-MB-231 triple-negative breast cancer cell; Mannose mediate cancer targeting; Electrochemical impedance cyto-sensor; Acidic tumor microenvironment, Stimuli-active drug release

REFERENCES

- [1] Tang, Y.-H.; Lin, H.-C.; Lai, C.-L.; Chen, P.-Y. *. Mannosyl electrochemical impedance cytosensor for label-free MDA-MB-231 cancer cell detection. *Biosens. Bioelectron.* **2018**, 116, 100-107.
- [2] Liang, W.; Chen, Z.-J.; Lai, C.-H.* Fabrication of a reusable electrochemical platform based on acid-responsive host-guest interaction with β -cyclodextrin. *Carbohydrate Research* **2023**, 534, 108966.
- [3] Li, H.-Y.; Lin, H.-C.; Huang, B.-J.; Lo, A. Z. K.; Saidin, S.; Lai, C.-H.*; Size Preferences Uptake of Glycosilica Nanoparticles to MDA-MB-231 Cell. *Langmuir* **2020**, 36(38), 11374-11382.
- [4] Su, Y.-H.; Lin, H.-C.; Li, H.-Y.; Lien, C.-H.; Shih, Y.-H.; Lai, C.-H.*; Mannoside-Functionalized Silica Nanocomposite-Encapsulated Doxorubicin for MDA-MB-231 Cancer Cell Targeting and Delivery. *ACS Applied Nano Materials* **2023**, 6, 4957-4968.
- [5] Wu, T.-C.; Lai, C.-L.; Sivakumar, G.; Huang, Y.-H.; Lai, C.-H.*; Synthesis of a Multifunctional Glyco-Block Copolymer through Reversible Addition–Fragmentation Chain Transfer Polymerization and Click Chemistry for Enzyme and Drug Loading into MDA-MB-231 Cells. *ACS Appl. Mater. Interfaces* **2023**, 15, 59746-59759.

No. O-3

Microstructure and Microwave Dielectric Properties of Low-Temperature Sintering $Mg_{2-x}Mn_xV_2O_7$ Ceramic for 5G communication components

Zhong-Hao Wang^{†,1}, Yong-Tai Xu¹, Che-Hao Liao¹, Chia-Hung Chang², and Shih-Hung Lin^{*,1}

¹ Department of Electronic Engineering, National Yunlin University of Science and Technology, Taiwan

² Department of Electrical Engineering, National Yunlin University of Science and Technology, Taiwan

[†]Presenter

^{*}Corresponding author's e-mail: isshokenmei@yuntech.edu.tw

ABSTRACT

In recent years, wireless communication has increased, 5 G communication products not only pursue light, thin, short, and small sizes but also need high speed, low latency, and massive connectivity. As a result, the Low-Temperature Co-fired Ceramics (LTCC) technology has become the principal process of microwave dielectric because of its excellent dielectric properties and low cost.

This experiment is divided into two parts. The first part proposes a novel LTCC material [1] and attempts to explore its microwave dielectric properties by changing the process parameters. The second part designs a bandpass filter using electromagnetic simulation software and implements it using the best LTCC material developed in the first part.

First, the solid-state reaction method is used to replace Manganese (Mn^{2+}) for magnesium (Mg^{2+}) in $Mg_2V_2O_7$ dielectric material to form $Mg_{2-x}Mn_xV_2O_7$ the experimental discussion on the relationship between the dielectric and physical properties of the material [2]. The $Mg_{1.725}Mn_{0.275}V_2O_7$ ceramics sintered at 920 °C for 5h has an $\epsilon_r = 9.7$, $Q_f = 47,400$ (GHz), and $\tau_f = -9.72$ (ppm/°C). Since the τ_f value is already less than -10 ppm/°C, there is no need to add other materials with high positive temperature coefficients to bring τ_f near zero. Therefore, it has great potential as a substrate material for low-temperature co-fired ceramics and can be used in the implementation to relate wireless communication components.

Finally, a 5G bandpass filter was designed using electromagnetic simulation software [3]. The filter parameters were simulated using the novel LTCC material developed in the first part to verify its difference from other commercial substrates.

Keyword: LTCC; Ceramic Material; Communication Components; Dielectric Properties

REFERENCES

- [1] Moyan Zang, Mupeng Zheng, Mankang Zhu, Yudong Hou, Low-temperature sintering and microwave dielectric properties of $CaMoO_4$ ceramics for LTCC and ULTCC applications, Journal of the European Ceramic Society, Volume 44, Issue 1, 2024, Pages 293-301,ISSN 0955-2219, <https://doi.org/10.1016/j.jeurceramsoc>.(2023)
- [2] M. R. Joung, J. S. Kim, M. E. Song, and S. Nahm, "Formation and Microwave Dielectric Properties of the $Mg_2V_2O_7$ Ceramics," Journal of the American Ceramic Society., vol 92, Issue 7, December 2009, Pages 1621-1624.
- [3] B. W. Hakki and P. D. Coleman, IEEE Trans. Microwave Theory Technol., 8, 402 (1960).

No. O-4

TITLE: Microwave dielectric properties of $\text{CaTi}_{1-x}(\text{Co}_{1/3}\text{Nb}_{2/3})_x\text{O}_3$ for applications in high-frequency device

Yu-Hsuan Tseng^{†,1}, Jyun-Fong Lin¹, Che-Hao Liao¹, Chia-Hung Chang², and Shih-Hung Lin^{*,1}

¹ Department of Electronic Engineering, National Yunlin University Science and Technology, Taiwan

² Department of Electrical Engineering, National Yunlin University Science and Technology, Taiwan

[†]Presenter

*Corresponding author's e-mail: isshokenmei@yuntech.edu.tw

ABSTRACT

In recent years, the rapid growth of 5G communication and low-orbit satellites has driven the global communications industry. This study focuses on developing high-frequency components with fast transmission, low latency, and low cost, particularly the filter substrate. Current commercial high-frequency substrates are suspected to have high losses, making it essential to develop ultra-low-loss microwave dielectrics for improved filter performance[1].

In this study, the B-site substitution of CaTiO_3 to form $\text{CaTi}_{1-x}(\text{Co}_{1/3}\text{Nb}_{2/3})_x\text{O}_3$ dielectric was carried out by solid-state reaction method, and the dielectric properties were investigated under the conditions of $x=0.1-0.7$, and the sintering temperature of 1400-1500 °C. The electrical properties were verified by XRD, SEM, EDS, Density, Raman, and other physical analyses. The experimental results show that the highest $Qf = 42,400$ (GHz), $\epsilon_r = 95.1$, and $\tau_f = 259$ can be obtained at the sintering temperature of 1475 °C, periods for 3 hours, and $x = 0.2$. According to the above results, the higher temperature drift makes it suitable for temperature compensators, but the quality factor is too low, which leads to high loss and, therefore, far from being sufficient for commercial substrates; therefore, the most common negative drift will be utilized in the present study.

Consequently, in this study, the most common negative Temperature coefficient of resonant frequency, MgTiO_3 , is mixed with $\text{CaTi}_{1-x}(\text{Co}_{1/3}\text{Nb}_{2/3})_x\text{O}_3$ to bring the temperature drift to zero and increase the Qf to about 93,800[2]. The excellent dielectric properties of the mixed-phase dielectric make it more suitable for 5G Sub-6, millimeter-wave communication systems, and low-orbit satellite systems. Finally, A self-designed Wide Stopband Microstrip Bandpass Filter was realized using this best dielectric parameter and verifies its improvement in microwave device performance compared to commercial substrates.

Keyword: Microwave dielectric; Positive temperature coefficient; Perovskite structure

REFERENCES

- [1] S.H. Lin, Z.Q. Lin, C.W. Chen, *Ceram. Int.*47 (2021)
- [2] C.L. Huang, C.L. Pan, S.J. Shium, *Liquid phase sintering of $\text{MgTiO}_3\text{-CaTiO}_3$ microwave dielectric ceramics*, *Mater. Chem. Phys.*, 78 (2003) 111-115.

No. O-5

TITLE: UV detector fabricated using ZnO thin film prepared by RF magnetron sputtering with a raw powder target

Wei-Cheng Pan[†], Lin-Yi Tang, Che-Hao Liao, and Chien-Sheng Huang*

Department of Electronic Engineering, National Yunlin University of Science and Technology, Yunlin 64002, Taiwan

[†]Presenter

*Corresponding author's e-mail: liaoeh@yuntech.edu.tw

ABSTRACT

UV detectors have been widely used in various applications, including civilian medicine, UV radiation monitoring, water treatment, flame detection, UV curing processes, and military facilities. These detectors are well-established and highly popular, garnering public interest. ZnO has been extensively researched as a potential photoelectric sensing material due to its wide bandgap, low cost, strong radiation resistance, and high chemical stability. In this study, we explored ZnO-based UV photoelectric sensors and enhanced their electrical properties by incorporating other materials into the ZnO powder target to improve their sensing performance.

In this study, we deposited ZnO onto sapphire substrates using radio frequency magnetron sputtering. The target material was a self-fabricated ZnO powder, sintered at 900°C. Future research could incorporate additional materials into the target to further enhance the electrical properties of ZnO. A ZnO layer with a thickness ranging from 200 to 500 nm was deposited under a controlled environment, introducing 40 mTorr of argon gas during the deposition process. The sputtering RF power was set to 200W, and the substrate temperature was maintained at 400°C to ensure optimal deposition conditions. Following deposition, the ZnO thin films underwent annealing in ambient air at temperatures ranging from 500°C to 800°C for a duration of 4 hours. This high-temperature annealing process was critical for improving the film's crystalline structure and electrical properties. After annealing, photolithography created an interdigital electrode pattern on the ZnO film. An aluminum (Al) electrode was then deposited via sputtering, followed by a lift-off process to complete the fabrication of the UV photodetector.

The device's performance was evaluated by measuring its photocurrent and dark current to assess its sensitivity to ultraviolet radiation. Electrical analysis was conducted to further understand the photodetector's characteristics and response under different conditions. Incorporating other materials into the ZnO powder target is recommended for future studies, as this approach could further enhance the electrical properties of the ZnO thin films. Optimizing these parameters, such as self-made sputtering target, deposition conditions, and annealing process, can improve the device's UV illumination sensitivity, making it suitable for various applications.

The ZnO UV photodetector, with a self-made sputtering target, exhibited significantly enhanced sensitivity. Compared to using pure ZnO alone, including additional materials will lead to marked improvements in electrical performance. This enhanced sensor holds great potential for a wide range of applications and can be adapted to meet various needs in daily life. Keyword: First-principles study, adsorption energy, triazole molecules, chemical mechanical polishing, chemical mechanical planarization

Keywords: Sapphire; ZnO; UV detector; Powder target

REFERENCES

- [1] Su-Shia Lin, Jow-Lay Huang. Effect of thickness on the structural and optical properties of ZnO films by r.f. magnetron sputtering. *Surf. Coat. Technol.*, **2004**, 185, 222-227.
- [2] Mariem Chaari, Adel Matoussi, Zouheir Fakhfakh. Structural and Dielectric Properties of Sintering Zinc Oxide Bulk Ceramic. *Materials Sciences and Application*, **2011**, 2, 765-770.

No. O-6

TITLE: Enhancing Field of View in 3D Floating Holographic Display Using Multiple LCoS-SLMs

Hao-Ming Kuo[†], Jyun-Yan Luo, Cang-Ci Guo, and Chun-Wei Tsai^{*}

Department of Electronic Engineering, National United University

[†]Presenter

^{*}Corresponding author's e-mail: cwtsai@nuu.edu.tw

ABSTRACT

A reflective-type Liquid Crystal on Silicon Spatial Light Modulator (LCoS-SLM) is a powerful optical instrument used to modulate the optical wavefront and has been widely applied in various applications and integrations in display and holography research. Examples include holographic projection displays [1], holographic displays [2], holographic near-eye displays [3], augmented reality, virtual reality, and automotive head-up displays (HUD). Additionally, the LCoS-SLM device features small pixels, a higher aperture ratio, and a thinner cell gap. These properties enhance the LCoS-SLM's diffraction angle, light efficiency, and response speed. Specifically, phase-only LCoS-SLM enables holographic displays to project images at variable focal lengths. Leveraging the functionality of LCoS-SLM, researchers can further extend these capabilities by incorporating true per-pixel focal depth, complex full-color shaded imagery, faster real-time calculations, more advanced aberration and vision correction, significantly wider fields of view, and more compact form factors.

In this paper, we developed a 3D floating holographic display for near-eye applications. A single 4K x 2K LCoS-SLM device struggles to provide a large viewing angle for both eyes at close distances. Therefore, we employed three 4K x 2K LCoS-SLM devices to expand the viewing angle to 36.67 degrees. The combined LCoS-SLM panel size, achieved using a beam splitter, forms a 12K x 2K LCoS-SLM. This work demonstrates a successful application of phase-only LCoS-SLM technology in holographic displays and near-eye applications, including augmented reality (AR) and virtual reality (VR).

Keywords: Spatial Light Modulator (SLM); 3D Floating Image; Holographic Display; Field of View (FOV)

REFERENCES

- [1] Hsu, W. F., Weng, M. H., "Compact holographic projection display using liquid-crystal-on-silicon spatial light modulator," *Materials*, **2016**, vol. 9, no. 9, 768.
- [2] J. P. Yang and H. M. Chen, "A 3-msec Response-Time Full-Phase-Modulation 1080p LCoS-SLM for Dynamic 3D Holographic Display," *SID Symposium Digest of Technical Papers*, 48 (1), **2017**, 1073-1076.
- [3] C. W. Tsai, F. Lin, and C. Wang, "Near Eye Application Based on Digital Electro-Optics Platform (X-on-Silicon)," *The 24th International Display Workshops (IDW'17)*, Sendai, Japan, December 6-8, **2017**.

No. O-7

TITLE: Interfacial Characteristics on the Joint of unidirectional Carbon fiber reinforced thermoplastics Composite /Aluminum alloy laminate

Ming-Yuan Shen^{*}, Chih-Hsien Cheng[†], and Shin-Yu Chen

Department of Mechanical Engineering, National Chin-Yi University of Technology, Taiwan

[†]Presenter

^{*}Corresponding author's e-mail: hbj678@gmail.com

ABSTRACT

Since carbon fiber reinforced plastics (CFRP) are lighter than metals and have high strength, modulus, and other properties, they are commonly used in transportation vehicles. However, due to material costs and economic factors, complete substitution with carbon fiber composites is often impractical. In practical applications, CFRP are frequently combined with other lightweight metal materials to create fiber/metal laminates. Using polyamide 66 as thermoplastic matrix, this study optimizes the production of unidirectional carbon fiber prepreg (Tow prepreg, Towpreg). First, the aluminum alloy surface was modified with the modifier to enhance the interface between the alloy and the resin; this is the covalent bonding that results in glue-free joining. Following that, the towpreg was placed on the alloy surface and bonded using Automated fiber placement (AFP) process. In order to create fiber/metal laminates (FML), two dissimilar materials are subsequent joined using hot pressing. The characteristics of FMLs were investigated in this study.

It can enhance the interface between the alloy and towpreg when the specimens are modified on the aluminum alloys. As compared to the unmodified joints, modified joints showed significant improvement in tensile strength.

Keyword: Thermoplastic resin; Unidirectional carbon fiber prepreg; Process optimization; Carbon fiber metal laminate; Joining of dissimilar materials

REFERENCES

- [1] Fan, Q., Duan, H., & Xing, X. (2024). A review of composite materials for enhancing support, flexibility and strength in exercise. *Alexandria Engineering Journal*, 94, 90-103.
- [2] Yao, S. S., Jin, F. L., Rhee, K. Y., Hui, D., & Park, S. J. (2018). Recent advances in carbon-fiber-reinforced thermoplastic composites: A review. *Composites Part B: Engineering*, 142, 241-250.
- [3] Dirk, H. J. L., Ward, C., & Potter, K. D. (2012). The engineering aspects of automated prepreg layup: History, present and future. *Composites Part B: Engineering*, 43(3), 997-1009.
- [4] Wilhelm, W., Stephen, R. H., Mike, I. J., Moritz, K., Andreas, H., & Maik, G. (2018). Experimental investigation of the effect of defects in Automated Fibre Placement produced composite laminates. *Composite Structures*, 201, 1004-1017.
- [5] Nathaniel, H., Pratik, K., Timothy, Y., Anahita, E., & Mehran, T. (2023). In situ consolidation of carbon fiber PAEK via laser-assisted automated fiber placement. *Composites Part B: Engineering*, 249, 110405.
- [6] Kim, S. Y., Lim, T. W., Sottos, N. R., & White, S. R. (2019). Manufacture of carbon-fiber prepreg with thermoplastic/epoxy resin blends and microencapsulated solvent healing agents. *Composites Part A: Applied Science and Manufacturing*, 121, 365-375.
- [7] Kirill, M., Sergey, G., Anastasiia, R., Artem, T., Mariia, D., & Alexander, S. (2023). Pultrusion of thermoplastic composites with mechanical properties comparable to industrial thermoset profiles. *Composites Communications*, 44, 101766.
- [8] Hongfu, L., Yang, W., Chenwei, Z., & Boming, Z. (2016). Effects of thermal histories on interfacial properties of carbon fiber/polyamide 6 composites: Thickness, modulus, adhesion and shear strength. *Composites Part A: Applied Science and Manufacturing*, 85, 31-39.
- [9] Li, W., Geng, P., Wang, Q., Ma, N., Zhao, S., & Chen, C. (2023). Effect of thermal condition on isothermal-pressing joined strength of silanized Al alloy/carbon fiber-reinforced polyamide-6. *Journal of Materials. Research and Technology*, 24, 8035-8052.
- [10] Eri, O., Tomoki, M., Hiroto, S., Tomo, O., Fumikazu, M., Tomokazu, S., Mitsuru, O., & Akio, H. (2021). Friction stir spot welding of aluminum and carbon fiber reinforced thermoplastic using hybrid surface treatment improving interfacial properties. *Materials & Design*, 212, 110221.

- [11] Ma, H., Zhao, Y., Qin, G., & Geng, P. (2022) . Formation of nanoscale reaction layer with several crystallinities in the friction-welded 6061 Al alloy/steel joint. *Materials & Design*,219,110742.
- [12] Geng, P., Ma, H., Li, W., Murakami, K., Wang, Q., Ma, N., Aoki, A., Fujii, H., & Chen, C.(2023).Improving bonding strength of Al/CFRTP hybrid joint through modifying friction spot joining tools. *Composites Part B: Engineering*, 254,110588.
- [13] Guo, Y., Zhao, H., Zhai, D., Gao, Z., Li, Q., Chen, X., & Zhao, G. (2023) . Micro/nano dual-scale porous surface structure of the Al alloys and improvement on the joint strength with carbon fiber reinforced PA 6 thermoplastic. *Composites Part B: Engineering*,249, 110407.
- [14] Zhou, C., Li, Y., Zhu, G., Luo, G., Zhao, X., & Yu, Q.(2021) . Tensile and flexural behavior of metal/CFRP hybrid laminated plates. *Polymer Composites*,42,2882-2897.
- [15] Chen, J., Fu, K., & Li, Y. (2021). Understanding processing parameter effects for carbon fibre reinforced thermoplastic composites manufactured by laser-assisted automated fibre placement (AFP). *Composites : Applied Science and Manufacturing*,140,106160.

No. O-8

TITLE: AlN SAW Humidity Sensing Enhancement with SiO₂ Nanoparticles

Lu-Xiang Wang, Zhong-Hong Yen, Che-Hao Liao[†], Shih-Hung Lin, and Chien-Sheng Huang^{*}

Department of Electronic Engineering, National Yunlin University of Science and Technology, Yunlin 64002, Taiwan

[†]Presenter

^{*}Corresponding author's e-mail: huangchs@gmail.yuntech.edu.tw

ABSTRACT

Surface Acoustic Wave (SAW) devices have found applications in wireless communication and hold potential for a wide range of sensing applications [1]. Nanoparticles were selected as the material for this experiment due to their high specific surface area and ability to adsorb water molecules. In contrast, AlN is considered a promising material for SAW due to its exceptional piezoelectric properties and high speed of sound. In this study, we investigated the concentration of nanoparticles within the sensing area of AlN SAW devices to combine these two materials and enhance their sensing capabilities.

Subsequently, the photolithography technique was utilized to imprint 30 sets of interdigital transducers (IDTs) with a spacing of 10 μm , composed of aluminum electrodes onto the AlN/c-plane sapphire substrate. In the sensing region, By using the spin-coating method, nanoparticles are uniformly distributed across the sensing layer, and the microstructure of this region was examined via scanning electron microscopy (SEM). We delved into the impact of varying nanorod shapes on the overall device performance. Furthermore, we assessed the humidity-sensing characteristics of these devices using a vector network analyzer.

The research findings indicate that adjusting the ratio of alcohol to nanoparticles affects the concentration of nanoparticles in the dispersant. This alteration leads to changes in the nanoparticles attached to the sensing layer, which in turn influences the frequency shift of the device's central frequency. Specifically, when the alcohol-to-nanoparticle ratio is 1:1, the frequency shift reaches 487 kHz, with a sensitivity of 6.08 kHz/%RH. In comparison to devices without nanoparticles, this sensitivity represents an increase of 2.31 times (Δf : 210 kHz, S: 2.62 kHz/%RH). Furthermore, the device exhibited a response time of 180 seconds and a recovery time of 110 seconds in an environment with 10%-90% relative humidity (RH), which is 2.14 times longer than that of devices lacking nanoparticles. This suggests that while nanoparticles can enhance the device's sensitivity, they also prolong both the response and recovery times.

The AlN SAW humidity sensor, which incorporates nanoparticles in the sensing layer, demonstrates exceptional sensitivity, showing an improvement of 2.31 times compared to devices that do not utilize nanoparticles. However, the response and recovery times increase by 2.41 times, enhancing its versatility for a broad spectrum of applications, including but not limited to liquid and biosensing applications.

Keyword: AlN; SAW; SiO₂ Nanoparticles; Humidity sensor

REFERENCES

- [1] D. Mandal; S. Banerjee. Surface Acoustic Wave (SAW) Sensors: Physics, Materials, and Applications. *Sensors* **2022**, Volume 22, pp. 820.

No. O-9

TITLE: PVDF-Muscovite bimorph system as flexible transparent thermal sensor

Ching-Ming Su^{†,1}, Jyh-Ming Wu², Che-Ning Yeh², Ying-Hao Chu^{*,2}

¹ Department of Materials Science and Engineering, National Yang Ming Chiao Tung University, Hsinchu, Taiwan

² Department of Materials Science and Engineering, National TsingHua University, Hsinchu, Taiwan

[†]Presenter

^{*}Corresponding author's e-mail: yhchu@mx.nthu.edu.tw

ABSTRACT

With the rise of wearable devices, research on flexible materials has become more crucial. However, moderating the connection of multiple functions and the interaction between humans and devices is essential. Thus, the actuators and sensors become significant components in this field. This study focuses on improving the sensitivity of flexible thermal sensors to follow up on the human body's condition. We propose a thermally sensitive system based on polyvinylidene difluoride (PVDF) and muscovite. Muscovite offers a platform for better thin film growth and stable mechanical flexibility in this system. The disparity in the coefficient of thermalexpansion between muscovite and PVDF is enormous, leading to a considerable strain under a low-temperature variation. Further, PVDF is a piezoelectric material that exhibits electric polarization variations due to the internal generation of mechanical stress, producing an electric field. With a thickness of 20 μ m, this system can generate an output voltage of up to 2.21V at a 100OC temperature variation. On the other hand, the transparency of PVDF /muscovite shows excellent potential for more applications, such as all-transparent wearable devices. In conclusion, considerable sensitivity can be achieved in the designed system. The subtle fluctuations of temperature can be detected daily and generate a considerable electric signal compared with a pyroelectric system. The measurement shows an effective pyroelectric coefficient of about 119.4 (10⁻⁴ C · m² · K⁻¹). Therefore, this research gives us an excellent option for integration into wearable devices.

Keyword: Muscovite; Flexible device; Thermal sensor; PVDF; Piezoelectric effect

No. O-10

TITLE: Research on U-Net thyroid nodule segmentation based on attention mechanism

Shi-Hong Qiu^{†,*1}, Cheng-Mu Tsai¹, and Chuan-Wang Chang²

¹ Graduate Institute of Precision Engineering, National Chung Hsing University, Taiwan

² Department of Computer Science and Information Engineering, National Chin-Yi University of Technology, Taiwan

[†]Presenter

*Corresponding author's e-mail: g112067010@mail.nchu.edu.tw

ABSTRACT

Thyroid nodules are a common clinical problem, and their incidence increases with age. Early diagnosis of malignant nodules is crucial to prevent further spread of cancer and improve patient survival rates. Therefore, it is crucial to develop an efficient and accurate thyroid ultrasound nodule segmentation technology.

In this study, we focus on developing a thyroid nodule segmentation technology based on advanced deep learning technology. The main method is to use the U-Net [1] model as the basic architecture. In addition, we also introduce ResNet50 [2] as the backbone network of U-Net, which is a network architecture based on residual learning that can handle deeper feature learning problems and improve Model stability and performance. To further improve the performance of the model, we incorporate several advanced attention mechanisms. Among them, the squeeze and excitation network (SE) [3] strengthens the attention on key channels by adaptively adjusting the weight of each channel. Efficient Channel Attention Network (ECA) [4] uses lightweight one-dimensional convolution to capture the dependencies between channels, providing an efficient and accurate attention mechanism. The Convolutional Block Attention Module (CBAM) [5] combines two mechanisms, channel attention and spatial attention, to adjust feature maps at a more detailed level, further improving the detection performance of the model.

After experimental verification, the U-Net model combined with the attention mechanism shows higher accuracy and consistency in the segmentation task of thyroid nodule ultrasound images. Specific results show that the model's segmentation performance in detecting thyroid nodules on ultrasound images has improved.

This study successfully developed a U-Net model that combines multiple attention mechanisms for segmentation and detection of ultrasound images of thyroid nodules. In the thyroid nodule ultrasound imaging data set, mPA and mIoU reached 91.51 and 83.29 respectively, and have the potential to help doctors make more accurate diagnostic decisions in clinical applications. Future research will be dedicated to further optimizing this tool and extending its scope of application.

Keyword: Thyroid nodule segmentation; U-Net; Squeeze and Excitation Network (SE); Efficient Channel Attention Network (ECA); Convolutional Block Attention Module (CBAM)

REFERENCES

- [1] Ronneberger, Olaf, Philipp Fischer, and Thomas Brox. "U-net: Convolutional networks for biomedical image segmentation." *Medical image computing and computer-assisted intervention—MICCAI 2015: 18th international conference, Munich, Germany, October 5-9, 2015, proceedings, part III* 18. Springer International Publishing, **2015**.
- [2] He, Kaiming, et al. "Deep residual learning for image recognition." *Proceedings of the IEEE conference on computer vision and pattern recognition*. **2016**.
- [3] Hu, Jie, Li Shen, and Gang Sun. "Squeeze-and-excitation networks." *Proceedings of the IEEE conference on computer vision and pattern recognition*. **2018**.
- [4] Wang, Qilong, et al. "ECA-Net: Efficient channel attention for deep convolutional neural networks." *Proceedings of the IEEE/CVF conference on computer vision and pattern recognition*. **2020**.
- [5] Woo, Sanghyun, et al. "Cbam: Convolutional block attention module." *Proceedings of the European conference on computer vision (ECCV)*. **2018**.

No. O-11

TITLE: Optimization of Telecentric Lens Design Using Zemax for Precision Machine Vision

Ming-Ren Liu^{†,*} and Cheng-Mu Tsai

Graduate Institute of Precision Engineering, National Chung Hsing University, Taiwan

[†]Presenter

*Corresponding author's e-mail: g112067046@mail.nchu.edu.tw

ABSTRACT

This study aims to design and optimize a telecentric lens using Zemax. Telecentric lenses are crucial for high-precision instruments and machine vision systems, as they significantly reduce image distortion. The key feature of telecentric lenses is that the light rays remain parallel to the optical axis as they enter the camera, thereby enhancing measurement accuracy and consistency. At the initial stage of the design, we selected a combination of positive and negative lenses as the starting point, beginning with a small field of view and a large aperture, and gradually increasing the design complexity. As the design progressed, the lens system expanded from two lenses to five, eliminating aberrations and optimizing image quality. During this process, we systematically increased the field of view and aperture by continuously adjusting the curvature, thickness, and spacing of the lenses, aiming to maintain optical performance while achieving a larger field of view and smaller aperture. The ultimate goal is to design a high-performance telecentric lens with an f-number of 2, a magnification of 10X, and a maximum field angle of 8.8 degrees, suitable for precision measurement and industrial applications. Additionally, to ensure that the system meets the expected image quality, we set specific Modulation Transfer Function (MTF) requirements. MTF is a critical measure of the lens's resolution and image detail. We require the lens to meet the following MTF values at specific frequencies: at half the Nyquist frequency, the MTF should be greater than 0.3; at 0.45 times the Nyquist frequency, the MTF should exceed 0.4; and at 0.35 times the Nyquist frequency, the MTF should be higher than 0.5. Furthermore, we aim for smaller spot sizes to ensure better focusing and reduced aberrations, which will further enhance image clarity. In summary, by gradually increasing the number of lens elements and continuously optimizing the design in Zemax, this study aims to create a high-precision, distortion-free telecentric lens system for industrial and machine vision applications. The rigorous MTF standards ensure that the final system will meet high image quality requirements, making it suitable for applications requiring precise imaging over a large field of view.

Keywords: Telecentric lens design; Modulation Transfer Function (MTF) optimization; High-precision machine vision systems

REFERENCES

- [1] Choi, Hojong ,Cho, Seongil , Ryu, Jaemyung), "Novel Telecentric Collimator Design for Mobile Optical Inspection Instruments," *Current Optics and Photonics*, **2023**.
- [2] Miks, Antonin , Novak, Jiri, "Design of a double-sided telecentric zoom lens," *APPLIED OPTICS*, **2012**.
- [3] J. Gregory Hollows, Nicholas James "Telecentric Lens Size Control and Telecentric Design Topics,"Edmund Knowledge Center, **2020**.
- [4] Butkus, Bruce. "Telecentric Illumination for Vision-System Backlighting." *Machine Design*. June 2, **2009**. Accessed January 12, 2012.

No. O-12

TITLE: Design of Silicone Light Guide with Mini LED in Automotive Headlamps

Yu-Fu Hsu[†], Chia-Chun Hu, Yang-Jun Zheng, and Zhi-Ting Ye*

Graduate Institute of Opto-Mechatronics, Department of Mechanical Engineering, National Chung Cheng University, Taiwan

[†]Presenter

*Corresponding author's e-mail: imezty@ccu.edu.tw

ABSTRACT

Traditional car headlights typically use halogen or high-intensity discharge (HID) lamps, along with a reflector, fisheye lens, and shading plate to meet ECE112B regulations for asymmetric low beams. However, this design tends to be bulky and compromises optical efficiency due to the shading plate. This paper introduces a more compact solution for low-beam headlights by utilizing an LED light source and a Silicone Light Guide (SLG). By leveraging the principle of total internal reflection, the design confines the light beam within the silicone LG, reducing the headlight's size while optimizing its structure and improving light distribution [1].

Keyword: Headlights; High-intensity discharge; Fisheye lens; Silicone Light Guide

REFERENCES

- [1] Hu, C. C., Zheng, Y. J., Hsu, Y. F., & Ye, Z. T. (2024). Design and Application of Liquid Silicone Rubber Light Guide in Compact Automotive Headlamps. *International Journal of Optomechatronics*, VOL. 18, NO. 1, 2343407, <https://doi.org/10.1080/15599612.2024.2343407>.

No. O-13

TITLE: Application of Virtual Factory Environment Simulation in Safety Education Training

Chiao-Ling Lin^{†,1}, Shih-Hung Lin², and Yao-Chin Wang^{*,3}

¹ Department of Computer Science and Information Engineering, Cheng Shiu University

² Department of Electronic Engineering, National Yulin University of Science and Technology

³ Department of Computer Science and Information Engineering, Cheng Shiu University

[†]Presenter

^{*}Corresponding author's e-mail: autherkyn@gmail.com

ABSTRACT

Virtual factory education, leveraging the power of Unity and Oculus[1] virtual reality technology, offers a groundbreaking approach to skill development and knowledge acquisition in the industrial and manufacturing sectors. By immersing students or employees in a simulated factory environment[2], this innovative educational platform provides a hands-on experience that closely replicates real-world operations. Key advantages of virtual factory education include:

- **Realistic Simulation:** Students can engage in a highly realistic factory environment, gaining valuable insights into machine operations, assembly processes, and quality control procedures.
- **Enhanced Engagement:** The immersive nature of VR technology fosters active participation and a deeper understanding of complex industrial concepts.
- **Personalized Learning:** Virtual factory education allows for tailored learning experiences, catering to individual needs and learning styles.
- **Cost-Effective Training:** By eliminating the need for physical factory setups, virtual factory education offers a cost-effective and efficient training solution.
- **Practical Experience:** Students can gain practical experience in a safe and controlled environment, preparing them for real-world industrial challenges.

The applications of virtual factory education are vast, extending across industrial training, manufacturing, and maintenance fields. By providing a highly immersive and interactive learning experience, this innovative approach can significantly enhance the skill levels of students and employees, meeting the evolving demands of modern industry.

Keywords: Virtual Factory Education; VR Technology; Immersive Learning; Industrial Training

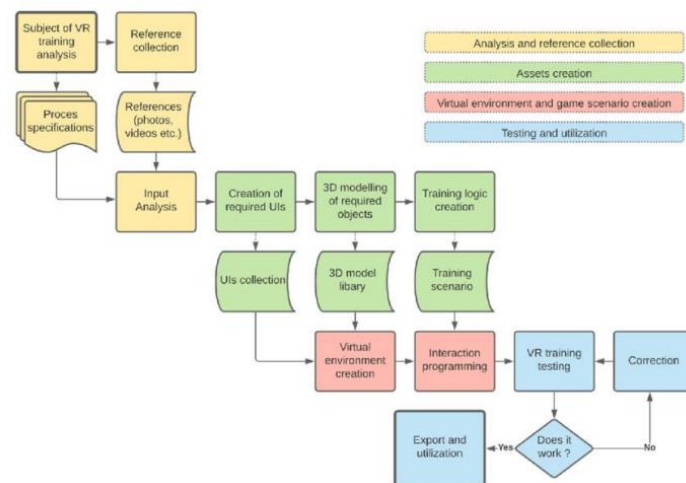


Fig.1 Illustrate the virtual factory environment simulation items.[2]

REFERENCES

- [1] Meta Quest Support. " How do I install the Oculus App on my PC?" YouTube, **2020**,
(<https://youtu.be/6Vt25t1I2VY?si=uRC3m-TDxXZozzLG>)
- [2] Krajčovič, Martin & Gabajová, Gabriela & Matys, Marián & Grznár, Patrik & Dulina, Ľuboslav & Kohar, Robert. (**2021**).
3D Interactive Learning Environment as a Tool for Knowledge Transfer and Retention. Sustainability. 13. 7916.
10.3390/su13147916.

No. O-14

TITLE: Silicon Photonics Switch with Electrostatic MEMS Actuator and Zero Power Consumption in Steady State

Jyun-Yan Luo[†], Wei-Siang Dai, Jin-Jia Ye, Chen-Yu Fu, and Chun-Wei Tsai*

Department of Electronic Engineering, National United University

[†]Presenter

*Corresponding author's e-mail: cwtsai@nuu.edu.tw

ABSTRACT

Optical signals, with faster transmission speeds than electrical ones, make silicon photonics an ideal fit for CMOS-compatible applications like quantum computing. However, the complexity and high costs of custom optical circuit design necessitate FPGA-like flexibility. A promising solution is a MEMS-based silicon photonic switch architecture with a non-volatile, Single-Pole Double-Throw (SPDT) switch using a MEMS phase shifter. This SPDT switch achieves three stable states through bistable mechanisms, making it effective for honeycomb lattice waveguides. By applying an electrostatic voltage to the actuator's electrodes, the input waveguide's position is adjusted, allowing precise control of the optical signal path across output waveguides.

Keyword: Photonics Integrated Circuits (PICs); Micro-Electro-Mechanical Systems (MEMS)

REFERENCES

- [1] Pierre Edinger, Alain Yuji Takabayashi, Carlos Errando-Herranz, Umar Khan, Cleitus Antony, Giuseppe Talli, Peter Verheyen, Wim Bogaerts, Niels Quack, and Kristinn B. Gylfason, "A Bistable Silicon Photonic Mems Phase Switch For Nonvolatile Photonic Circuits," *2022 IEEE 35th International Conference on Micro Electro Mechanical Systems Conference (MEMS)*, Tokyo, Japan, **2022**, pp. 995-997
- [2] Alain Yuji Takabayashi, Hamed Sattari, Pierre Edinger, Peter Verheyen, Kristinn B. Gylfason, Wim Bogaerts, and Niels Quack, "Broadband Compact Single-Pole Double-Throw Silicon Photonic MEMS Switch," in *Journal of Microelectromechanical Systems*, vol. 30, no. 2, pp. 322-329, April **2021**
- [3] Yashar Gholami, Kian Jafari, Mohammad Hossein Moaiyeri, "A novel bistable optical phase shifter using non-volatile MEMS actuator for application in photonic integrated circuits," *Optics Communications*, vol. 574, pp. 131119, **2025**

No. O-15

TITLE: A Mach-Zehnder Modulator with One-Dimensional Photonic Crystal Filter and Integrated Liquid Crystal Material

Cang-Ci Guo[†], Hao-Ming Kuo, Yu-Sheng Kan, Zhi-Xiang Huang, and Chun-Wei Tsai*

Department of Electronic Engineering, National United University

[†]Presenter

*Corresponding author's e-mail: cwtsai@nuu.edu.tw

ABSTRACT

The Mach–Zehnder interferometer (MZI) is used to detect relative phase shifts between two collimated beams that are produced by splitting light from a single source[1]. A photonic crystal is an optical nanostructure where the refractive index changes periodically[2]. We designed a one-dimensional photonic crystal structure on a surface that functions as a filter, creating a bandgap in a specific propagation direction. Liquid crystals exhibit electrically controlled birefringence, where applying different voltages changes their effective refractive index. In our approach, we integrate the photonic crystal structure with liquid crystal material and micro-electro-mechanical systems (MEMS) technology to develop MZI-based filters[3]. This design involves adjusting the radius of the columns within the photonic crystal and introducing defects to enable beam splitting and reflection. Furthermore, liquid crystals are embedded into the MZI path within the photonic crystal structure. The output spectrum of the structure is modulated by applying a controlled voltage, and we analyze how this impacts the system, establishing a theoretical link between the applied voltage and transmission wavelength. Simulations using the finite difference time domain (FDTD) method show that controlling the applied voltage alters the output transmission wavelength. As a result, the MEMS photonic crystal-based MZI interferometer filter can be implemented and used in optical wavelength division multiplexing (WDM) systems.

Keyword: Micro-Electro-Mechanical Systems(MEMS); Mach-Zehnder Interferometer(MZI); Wavelength Division Multiplexing (WDM); Photonics Crystal, Liquid Crystal

REFERENCES

- [1] M. Caño-García, D. Poudereux, F.J. Gordo, M. A. Geday, J. M. Otón, X. Quintana, “Integrated Mach–Zehnder Interferometer Based on Liquid Crystal Evanescent Field Tuning,” *Crystals*, vol. 9, no. 5, pp. 225, **2019**.
- [2] Integlia RA, Song W, Tan J, Jiang W., “Longitudinal and angular dispersions in photonic crystals: A synergistic perspective on slow light and superprism effects,” *J Nanosci Nanotechnol.*, vol. 10, no. 3, pp. 1596-605, **2010**.
- [3] T. Liu, F. Pagliano, R. van Veldhoven, V. Pogoretskii, Y. Jiao, and A. Fiore, “InP MEMS Mach-Zehnder Interferometer Optical Switch on Silicon,” 2019 *Conference on Lasers and Electro-Optics Europe & European Quantum Electronics Conference (CLEO/Europe-EQEC)*, **2019**.

No. O-16

TITLE: Performance Analysis and Optimization of Ship and Human Recognition in 2D Optical Radar Images Based on YOLOv7

Li-Lin Chen^{†,*} and Yao-Chin Wang

Department of Computer Science and Information Engineering, Cheng Shiu University

[†]Presenter

*Corresponding author's e-mail: barry1351413514@gmail.com

ABSTRACT

As global trade intensifies, increasing port throughput highlights ship navigation safety issues. Frequent accidents in busy waterways reveal limitations of existing monitoring systems. Traditional radar and visual sensing technologies struggle with environmental interference and precision challenges.

Researchers propose combining LiDAR (Light Detection and Ranging) with Artificial Intelligence (AI) to address these issues. This system offers high-precision environmental perception in various weather conditions. It collects precise 3D data using LiDAR and analyzes it with AI algorithms, accurately identifying vessels and obstacles while providing detailed environmental understanding.

The system's all-weather capability enhances safety management efficiency, enabling accurate judgments even in low visibility or night-time conditions. This advancement is expected to significantly reduce navigation accidents.

Integrating LiDAR and AI offers a new approach to longstanding shipping industry safety issues, laying the foundation for future intelligent shipping systems while enhancing navigational safety and optimizing port efficiency.

Keyword: LiDAR; Ship Detection; Maritime Safety

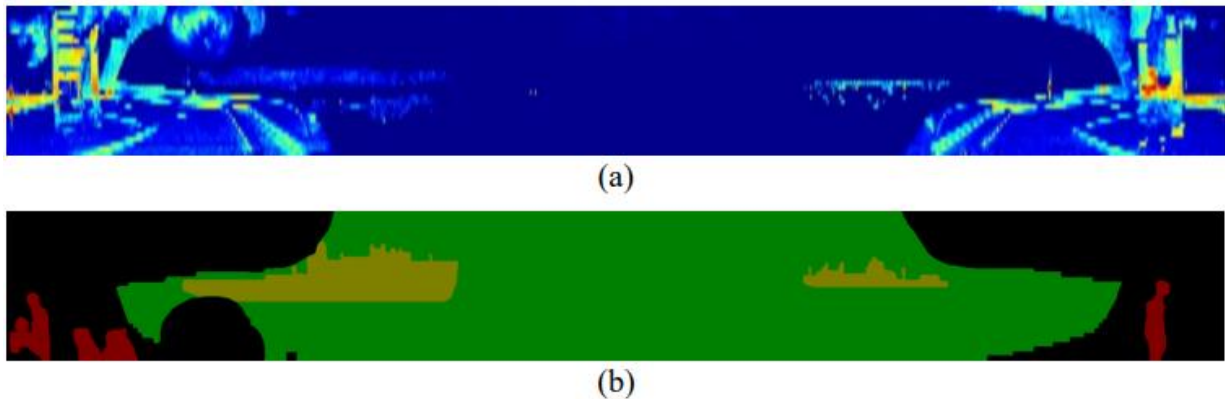


Fig.1 (a) original, (b) feature maps are upsampled via deconvolution, concatenated with the previous layer, and then fused through convolution for output.

REFERENCES

- [1] Lin, J.; Campa, G.; Framing, C.-E.; Gehrt, J.-J.; Zweigel, R.; Abel, D. Adaptive shape fitting for LiDAR object detection and tracking in maritime applications. *Int. J. Transp. Dev. Integr.* **2021**, *5*, 105-117.
- [2] Ibrahim, M.; Akhtar, N.; Ullah, K.; Mian, A. Exploiting Structured CNNs for Semantic Segmentation of Unstructured Point Clouds from LiDAR Sensor. *Remote Sens.* **2021**, *13*, 3621.
- [3] Zhang, L.; Wang, S.; Liu, R. YOLOv7-based ship detection and classification in maritime surveillance imagery. *IEEE Trans. Geosci. Remote Sens.* **2023**, *61*, 1-14.
- [4] Sun, Z.; Meng, C.; Huang, T.; Zhang, Z.; Chang, S. Marine ship instance segmentation by deep neural networks using a global and local attention (GALA) mechanism. *Plos One* **2023**, *18*, e0279248

No. P-1

TITLE: Enhancing the bending strength of polylactic acid biomedical polymer rods using ultrasound-assisted continuous drive friction welding

Chil-Chyuan Kuo^{*,1,2} and Hong-Wei Chen^{†,3}

¹ Department of Mechanical Engineering, Ming Chi University of Technology

² Research Center for Intelligent Medical Devices, Ming Chi University of Technology

³ International Ph. D. Program in Innovative Technology of Biomedical Engineering and Medical Device, Ming Chi University of Technology

[†]Presenter

*Corresponding author's e-mail: jacksonk@mail.mcut.edu.tw

ABSTRACT

Polylactic acid (PLA) is widely employed to make medical devices. However, a large medical device usually needs to be split into multiple parts for printing and joined together when limited by the size of the additive manufacturing platform. Generally, nuts and bolts are often used in laboratories to join the printed parts into a large medical device. However, this joint method can easily cause bolts and nuts to loosen or fall off during the reciprocating motion of a large medical device. Therefore, studying the joining technology of printed parts into a large medical device has become an essential research topic. The main objective is to enhance the joint strength of polylactic acid (PLA) polymer rods using ultrasound-assisted rotary friction welding (UARFW). Remarkably, the proposed method in this study complies with sustainable development goals due to high energy efficiency and low environmental pollution. The bending strength of the welded parts can definitely improve because ultrasonics promote the molten material flow in the weld joint during UARFW. The improvement of the bending strength of the welded parts is related to the location of the ultrasonic oscillator. The optimal position of the ultrasonic oscillator in the Z-axis direction of the CNC lathe is 5 mm with the improvement of the bending strength by approximately 96% due to ultrasonics promote the molten material flow during UARFW. The fracture locations of welded components made with UARFW occur within the base material, indicating that the weld interface exhibits superior strength compared to the base material. The surface hardness of the weld interface increases up to 25.7% compared with the surface hardness of the weld interface of the welded parts when rotary friction welding is performed without ultrasonic-assisted micro-vibration.

Keyword: Polylactic acid; Biomaterial; Ultrasound-assisted rotary friction welding; Joint strength

REFERENCES

- [1] Hassan, A.J., Boukharouba, T. & Miroud, D. Concept of forge application under effect of friction time for AISI 316 using friction welding process. *Int J Adv Manuf Technol* 112, 2223–2231 (2021).
- [2] Yin, P.; Xu, C.; Pan, Q.; Zhang, W.; Jiang, X. Effect of Different Ultrasonic Power on the Properties of RHA Steel Welded Joints. *Materials* 2022, 15, 768.
- [3] Li, B.; Liu, Q.; Jia, S.; Ren, Y.; Yang, P. Effect of V Content and Heat Input on HAZ Softening of Deep-Sea Pipeline Steel. *Materials* 2022, 15, 794.
- [4] Lambiase, F., Grossi, V. & Paoletti, A. Effect of tilt angle in FSW of polycarbonate sheets in butt configuration. *Int J Adv Manuf Technol* 107, 489–501 (2020).
- [5] Delijaicov, S., Rodrigues, M., Farias, A. et al. Microhardness and residual stress of dissimilar and thick aluminum plates AA7181-T7651 and AA7475-T7351 using bobbin, top, bottom, and double-sided FSW methods. *Int J Adv Manuf Technol* 108, 277–287 (2020).

No. P-2

TITLE: *Ab initio* Studies of Work Function Changes of NO Adsorption on ZnGa₂O₄(111) Surface for Gas Sensors

Jhih-Hong Shao¹, Guan-Yu Chen^{†,1}, and Po-Liang Liu^{*,1,2}

¹ Graduate Institute of Precision Engineering, National Chung Hsing University, Taichung 40227, Taiwan

² Department of Applied Materials and Optoelectronic Engineering, National Chi Nan University, Nantou 54561, Taiwan

[†]Presenter

*Corresponding author's e-mail: pliu@dragon.nchu.edu.tw

ABSTRACT

This study utilizes first-principles calculations based on density functional theory to evaluate the adsorption of nitric oxide on various ZnGa₂O₄(111) surfaces: clean surfaces, surfaces doped with noble metals (Pt, Pd, Au, and Ag), and surfaces with oxygen molecules. The study investigates the change in work function of these surfaces. The results indicate that the highest work function change observed for nitric oxide adsorption on the clean ZnGa₂O₄(111) surface is +0.23 eV. Among the noble metals, the Ag-doped ZnGa₂O₄(111) surface exhibits the highest work function change of +0.35 eV. Furthermore, when nitric oxide adsorbs onto the surface of oxygen molecules on ZnGa₂O₄(111), it readily reacts with the oxygen molecules to form NO₂-like molecules. This reaction leads to the highest work function change of +0.54 eV and renders the ZnGa₂O₄(111) surface with oxygen molecules cleaner compared to ZnGa₂O₄(111) alone, resulting in a 2.33-fold improvement in surface-sensing nitric oxide sensitivity. In an oxygen environment, nitric oxide adsorbed on the Ag-doped ZnGa₂O₄(111) surface exhibits the highest work function change among all noble metals +0.50 eV. The interaction between NO molecules and oxygen molecules on the surface demonstrates that the oxygen vacancies formed by oxygen molecules in the ZnGa film contribute to enhancing the performance of the ZnGa₂O₄(111) surface for sensing nitrogen monoxide. Additionally, the Ag-doped ZnGa₂O₄(111) surface demonstrates an increased change in work function for sensing nitrogen monoxide.

Keyword: First-principles; ZnGa₂O₄ epilayer; Gas sensor; Nitric oxide; Work function changes; Density functional theory; Surface morphology

REFERENCES

- [1] Zuhara, S. & Isaifan, R. The impact of criteria air pollutants on soil and water: a review. *Journal of Environmental Science and Pollution Research* 4, 278-284 (2018).
- [2] McCleverty, J.A. Chemistry of nitric oxide relevant to biology. *Chemical Reviews* 104, 403-418 (2004).
- [3] Jia, C., Fan, W., Yang, F., Zhao, X., Sun, H., Li, P. & Liu, L. A theoretical study of water adsorption and decomposition on low-index spinel ZnGa₂O₄ surfaces: correlation between surface structure and photocatalytic properties. *American Chemical Society* 29, 7025-7037 (2013).
- [4] Wu, M.R., Li, W.Z., Tung, C.Y., Huang, C.Y., Chiang, Y.H., Liu, P.L. & Horng, R.H. NO gas sensor based on ZnGa₂O₄ epilayer grown by metalorganic chemical vapor deposition. *Scientific Reports* 9, 97459 (2019).
- [5] Hafner, J. *Ab initio* simulations of materials using VASP: Density-functional theory and beyond. *Journal of Computational Chemistry* 29, 2044-2078 (2008).

No. P-3

TITLE: Highly Sensitive Anti-Resonance Liquid Core Fiber Fabry-Perot Interferometer

Han-Wei Xie[†], Bing-Qiu Lai, and Cheng-Ling Lee^{*}

Department of Electro-Optical Engineering, National United University, Miaoli 360, Taiwan

[†]Presenter

^{*}Corresponding author's e-mail: cherry@nuu.edu.tw

ABSTRACT

The optical guidance mechanism of a hollow-core fiber (HCF) can be explained based on the antiresonant reflecting optical waveguide (ARROW) model. Under this condition, when the wavelengths are close to the resonant wavelengths (λ_m), the high refractive index (RI) cladding is regarded as a Fabry-Perot etalon[1-2]. The wavelengths that satisfy the resonant condition of Fabry-Perot interference that would radiate through the HCF cladding are regarded as leaky modes. Additionally, in cases where the wavelengths deviate from the λ_m , the cladding reflects other optical waves [3-4].

This study proposes an anti-resonant Fabry-Pérot fiber interferometer (ARFPFI) utilizing a liquid-filled hollow-core fiber (HCF) for reflecting guidance. The mentioned ARFPFI with the liquid filling into the core of the HCF is achieved by fusion splicing two sections of side-polished single-mode fiber (SMF) to generate two open channels for liquid filling. By polishing a part of the cladding of SMF to reduce its diameter from 125 μm to about 85 μm and then cleaving it into two sections [5]. A $L=0.2\text{cm}$ length of HCF with a diameter ($D=50\mu\text{m}$) segment was sandwiched between the two side-polished fibers by fusion splicing method, as shown in Fig.s 1(a) and 1(b). Then, one of the tiny openings in the end face of the HCF was filled with RI liquids with $n_D=1$ and $n_D=1.3$ (Cargille-liquid) by the duration of the capillary action. The RI of the filled liquids is lower than that of the cladding to achieve anti-resonance Fabry-Perot interference.

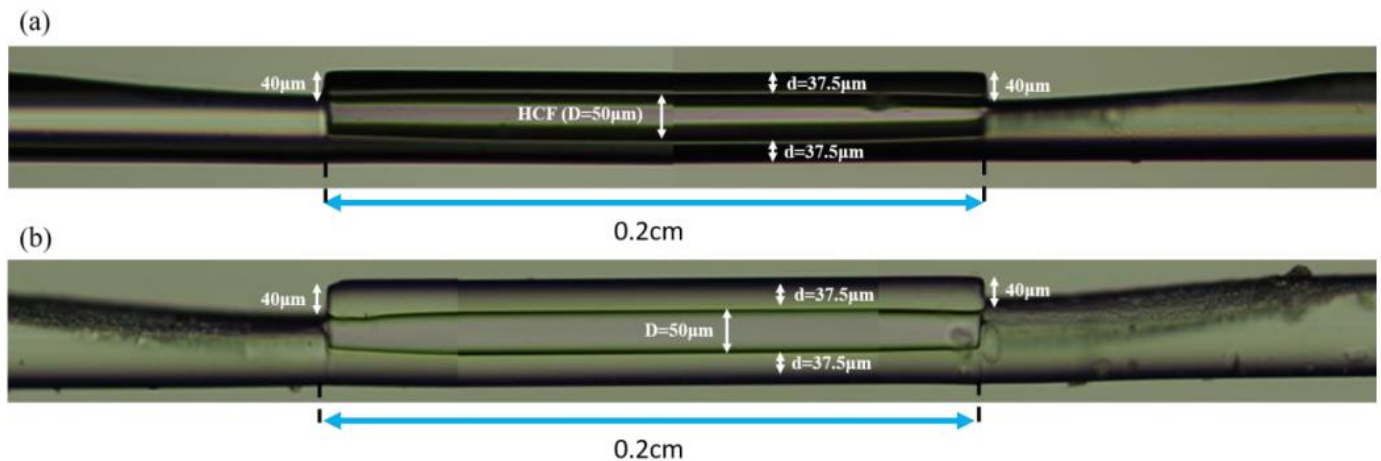


Fig.1 (a) Microscope grape of the anti-resonance Fabry-Perot fiber interferometer (ARFPFI) with $D=50\mu\text{m}$, and $L=0.2\text{cm}$. (b) Microscope grape of the ARFPFI filled with $n_D=1.3$ (Cargille-liquid)

Fig. 2 (a) and 2(b) show the optical interference spectra of the proposed ARFPFI filled with air and $n_D=1.3$ (Cargille-liquid). (c) The wavelength shifts with the filling liquid when the temperature is from 25°C to 45°C. We can observe that the wavelength shifts of the spectral interference at various temperatures are highly varied and results show the wavelengths red-shifted. That means the optical path difference in the Fabry-Perot interference mechanism increases. The temperature (T) sensitivity (S) can be shown in the following equation [4].

$$\frac{d\lambda_m}{dT} = \frac{2d}{m} \left(\frac{n_1}{\sqrt{n_1^2 - n^2}} \beta - \frac{n}{\sqrt{n_1^2 - n^2}} \alpha \right) \quad (1)$$

where d is the thickness of the HCF cladding; n and n_1 are the refractive indices of silica and the liquid core, respectively; α and β are the thermo-optic coefficients (TOC) of liquid core and silica, respectively. m is the resonance order.

Fig. 2 (d) by taking Eq. (1), At a selected wavelength around 1550 nm, the theoretical sensitivity (S) is calculated to be 1.64 nm/°C, while the experimental sensitivity (S) is measured at 1.57 nm/°C, showing a very similar agreement between the two values of experimental and theoretical.

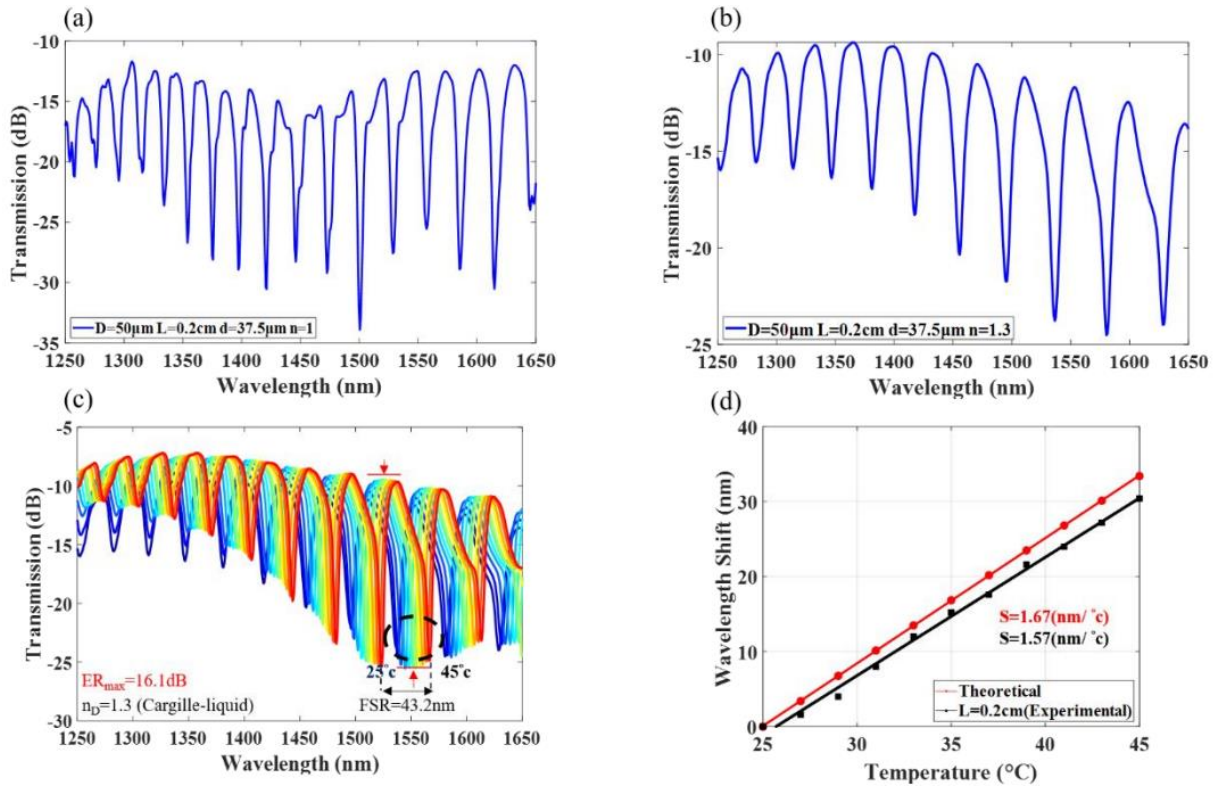


Fig. 2 Optical interference spectra of ARFPFIs filled with (a) air and (b) $n_D=1.3$ (Cargille-liquid), (c) interference responses by T variation, (d) sensitivities of the experimental and theoretical results.

Keyword: Anti-resonant reflecting optical waveguide (ARROW); Side-polished fiber; Anti-resonance Fabry-Perot fiber interferometer (ARFPFI); Liquid-core fiber

REFERENCES

- [1] Borwen, Y.; Lu, J. Y.; Yu, C. P.; Liu, T. A.; Peng, J. L. Terahertz refractive index sensors using dielectric pipe waveguides. *Opt. Lett.* **2012**, 20(06), 5858–5866.
- [2] Maoxiang, H.; Feng, Z.; Ying, W.; Yiping, W.; Changrui, L.; Shen, L.; Peixiang, Lu. Antiresonant reflecting guidance mechanism in hollow-core fiber for gas pressure sensing. *Opt. Lett.* **2016**, 24(24), 27890–27898.

- [3] Nian, C.; Li, X.; Ying, W. Multiplexing of anti-resonant reflecting optical waveguides for temperature sensing based on quartz capillary. *Opt. Lett.* **2018**,26(25), 33501–33509.
- [4] Shuangqiang, L.; Yingke, J.; Lugui, C.; Weimin, S.; Jun, Y.; Hanyang, L. Humidity-insensitive temperature sensor based on a quartz capillary anti-resonant reflection optical waveguide. *Opt. Lett.* **2017**,25(16), 18929–18939.
- [5] Linqing, Z.; Jieyuan, T.; Wenguo, Z.; Huadan, Z.; Heyuan, G.; Huihui, L.; Yaofei, C.; Yunhan, L.; Jun, Z.; Yongchun, Z.; Jianhui, Y.; Zhe, C. Side polished fiber: a versatile platform for compact fiber devices and sensors. *Photo. Sens.* **2023**, 13(1), 230120.

No. P-4

TITLE: Designs of a Badminton Training Assistant System with Recognition of Badminton Stroke Gestures by a Deep Learning Strategy of Dual-Modality Sensor Data of Both Imaging RGB and Wearable IMU

Ing-Jr Ding^{†,*}, Cheng-Feng Yang, Cheng-Yan Hu, and Bing-Cheng Gan

Department of Electronic Engineering, National United University No.2, Lienda, Miaoli 360302, Taiwan

[†]Presenter

*Corresponding author's e-mail: eugen.ding@gmail.com

ABSTRACT

In the sport industry, artificial intelligence (AI) is playing an important and indispensable role [1]. It's well-known that the smart watch in the current market can carry out sport gesture recognition in specific sport items (e.g., the popular Garmin swimming watch with recognized four main strokes). For the hot sport item of badminton [2], relatively much fewer studies focused on imports of deep learning-based AI techniques to assist the badminton player to build up a fine training plan involved with recognition of various badminton stroke gesture are explored. Aimed at this issue, this work develops a badminton training assistant system where swing motion-derived stroke gesture can be effectively recognized according to the clue of the player's action characteristics revealed by two different modalities of sensor data, "imaging RGB raw" and "wearable IMU raw." The badminton training assistant system developed in this work is a design of two separated recognition channels for performing gesture recognition of various shot actions made by the badminton player, which are the channel of convolutional neural network (CNN)-based deep learning computations with the input of the image data of RGB raw and the channel of long short-term memory (LSTM)-based deep learning estimates with the input of the wearable data of IMU raw [3-5]. For obtaining the image data of RGB raw, an image capture device, the RGB camera, is properly deployed in the playground; in acquisitions of the wearable data of IMU raw, a wearable device (mainly the use of the coin-sized board of 'MetaWearC' released by the laboratory of MBIENTLAB) is properly bound to the bottom of the grip of the badminton racket [6, 7]. To establish the training database to construct deep learning models of CNN with imaging RGB raw and LSTM with wearable IMU raw for stroke gesture recognition in an online sport exercise, a player with the expertise of the badminton sport is requested to take the specific badminton racket combined with the MetaWear board to make various classes of basic stroke actions in the camera-deployed playground. In the recognition channel by RGB raw sensing, two different frameworks of CNN models, TensorFlow-CNN using the library of JavaScript "TensorFlow.js" and YOLOv8 released by Ultralytics, are explored in classifications of sixteen badminton stroke gestures with considerations of shot action areas; in the LSTM stroke gesture recognition channel, six badminton stroke gestures without the shot action area issue are categorized, and for speeding up calculations, only the IMU raw of three-axis accelerator data is employed to establish the LSTM model. The developed badminton training assistant system in this work can significantly help the badminton player to achieve activity performance tracking and increase the expertise ability on the badminton sport.

Keyword: Badminton stroke gesture; Gesture recognition; Imaging RGB raw; Wearable IMU raw; Deep learning; Badminton training assistant system

REFERENCES

- [1] F. Wu et al., "A Survey on Video Action Recognition in Sports: Datasets, Methods and Applications," *IEEE Transactions on Multimedia*, vol. 25, pp. 7943-7966, **2023**, doi: 10.1109/TMM.2022.3232034.
- [2] C. Ma, D. Yu and H. Feng, "Recognition of Badminton Shot Action Based on the Improved Hidden Markov Mode," *Journal of Healthcare Engineering*, vol. **2021**, pp. 1-8, 2021, doi: 10.1155/2021/7892902.

- [3] TensorFlow-CNN, <https://www.tensorflow.org/js?hl=zh-tw>, retrieved on Oct. **2024**.
- [4] S. Rahman, J. H. Rony, J. Uddin and M. A. Samad, “Real-Time Obstacle Detection with YOLOv8 in a WSN Using UAV Aerial Photography,” *Journal of Imaging*, vol. 9, no. 10, pp. 216, **2023**, doi: 10.3390/jimaging9100216.
- [5] B. Lindemann, T. Müller, H. Vietz, N. Jazdi and M. Weyrich, “A Survey on Long Short-Term Memory Networks for Time Series Prediction,” *Procedia CIRP*, vol. 99, pp. 650-655, 2021, doi: 10.1016/j.procir.**2021**.03.088.
- [6] MetaWearC, <https://mbientlab.com/>, retrieved on Oct. **2024**.
- [7] J. Bort-Roig, E. Chirveches-Perez, F. Garcia-Cuyas, K. P. Dowd and A. Puig-Ribera, “Monitoring Occupational Sitting, Standing, and Stepping in Office Employees with the W@W-app and the MetaWearC Sensor: Validation Study,” *Jmir Mhealth and Uhealth*, vol. 8, no. 8, e15338, doi:10.2196/15338, **2020**.

No. P-5

TITLE: Reconstruction of Multimode Optical Fiber Transmission Images Using Pix2Pix GAN

Jin-Lin Wang^{†,1}, Hsu-Chih Cheng^{*,1}, and Chun-Ming Huang²

¹ Department of Electro-Optical Engineering, National Formosa University, Huwei, Yunlin 63201, Taiwan

² Department of Electronic Engineering, National Formosa University, Huwei, Yunlin 63201, Taiwan

[†]Presenter

^{*}Corresponding author's e-mail: chenghc@nfu.edu.tw

ABSTRACT

When laser carrying a message is transmitted through a multimode fiber (MMF), mode coupling and mode dispersion within the MMF produce a complex speckle pattern at the fiber's end, making image reconstruction a challenging task. In this study, we use the Pix2Pix GAN architecture to reconstruct the speckle images transmitted through multimode optical fiber using deep learning techniques. The experiment was conducted using the MNIST handwritten digit dataset, from which 10,000 speckle images were obtained after fiber optic transmission. These images were randomly divided into a training set and a test set for network training and testing. After the training was completed, the average structural similarity index (SSIM) of the reconstructed images was 0.56, with a maximum value of 0.78. Although the method is effective in reconstructing speckle images, there is still room for improvement. Future work could explore the performance of more complex neural networks and different optical fiber conditions.

Keyword: Multimode Fibre; Reconstruction of Speckle Images; Deep Learning; Pix2Pix Generates Adversarial Network

1. Introduction

Fiber optic technology has been widely used in endoscopic imaging [1][2]. Multimode fiber (MMF) significantly improves information transmission efficiency compared to single-mode fiber (SMF) because it can transmit a large number of modes simultaneously. However, during the transmission process in MMF, coupling and dispersion phenomena occur between the modes, ultimately resulting in an unrecognizable speckle pattern at the end of the fiber. To reconstruct images from these speckle patterns, several methods have been proposed by researchers, including transmission matrix [3], wavefront shaping [4], and digital phase [5], all of which have been shown to be effective in image reconstruction. However, these techniques require extremely precise control of the system and are sensitive to both the optical system and the imaging environment. Even minor changes in the scattering medium can have a significant impact on image quality.

To address these issues, many researchers have proposed a novel reconstruction method based on deep learning that overcomes the limitations of traditional methods, making image reconstruction more stable and consistent. Among them, convolutional neural networks (CNNs) have been widely applied to speckle image reconstruction [6][7]. To train CNNs, researchers need a large number of speckle image pairs as training data for end-to-end training. In this process, the neural network learns the correspondence between the input image and the labeled image without considering the structure of the optical system or the light propagation processes. The deep learning architecture used in this study is based on a 2016 paper by Phillip Isola et al. titled "Image-to-Image Translation With Conditional Adversarial Networks" [8].

2. Experimental Setup

The experimental setup is shown in Fig. 1. The incident light is a He-Ne laser (LSR532NL-100) with a wavelength of 532 nm. The laser beam first passes through a beam expander (magnification: 20) and an aperture to adjust the beam diameter, with a polarizer controlling the polarization direction. The beam is then directed to a spatial light modulator (SLM, JD955B Education Kit) where the MNIST handwritten digits

dataset is uploaded for transmission. After reflection by the SLM, the laser beam containing the image information passes through a beam splitter. One part of the beam is projected onto a CCD camera (HY-6210S) to inspect the reflected image from the SLM, while the other part is collected by a collimator and coupled into an optical fiber (2 m, 1000 μm , NA=0.22). Finally, the CCD at the fiber end collects the speckle images.

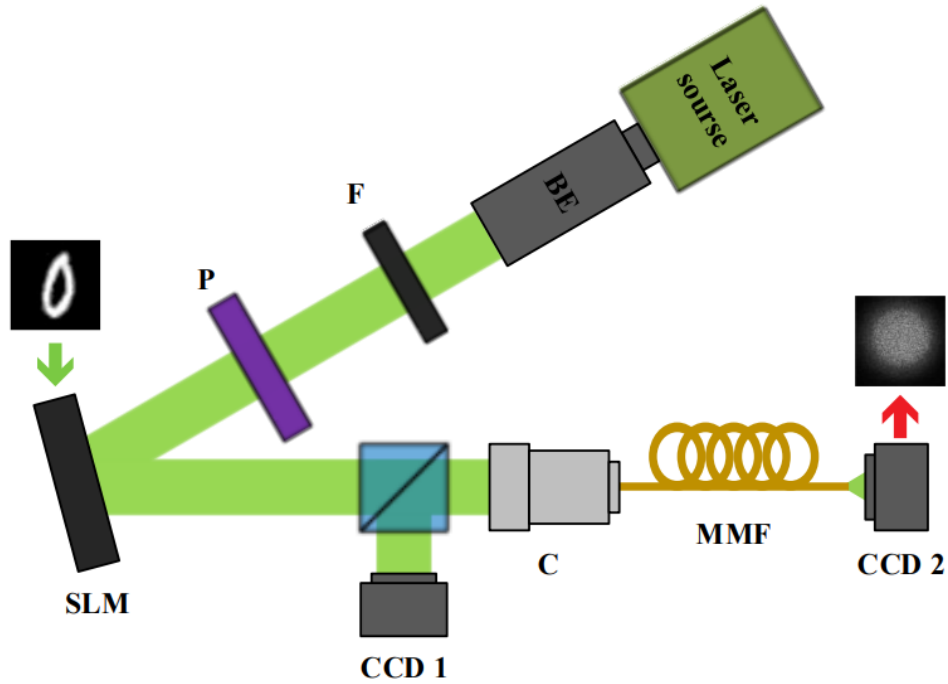


Fig. 1. Experimental setup for collecting speckle images. BE: beam expander, F: aperture, P: polarizer, SLM: spatial light modulator, BS: beam splitter, C: collimator, MMF:multimode fiber, CCD: camera.

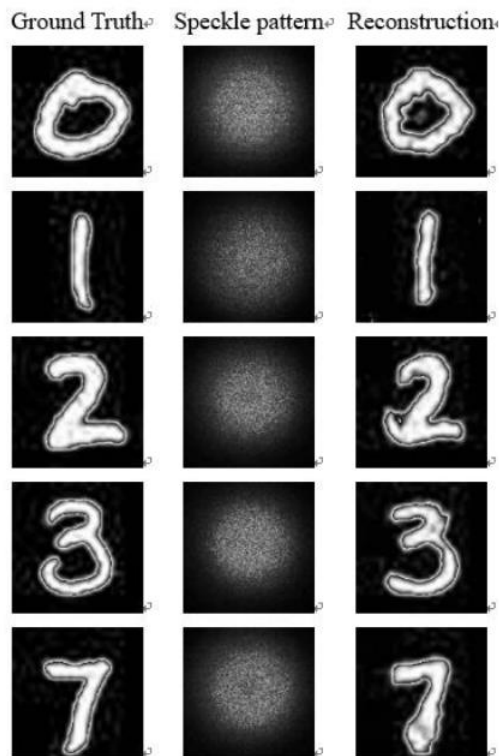


Fig. 2. Reconstruction results from deep learning. Ground Truth represents the original image, the Speckle pattern is the scattering image generated from the original image transmitted through MMF, and Reconstruction is the image obtained through deep learning reconstruction.

3. Experimental Results and Discussion

The images we used are from the MNIST handwritten digit dataset. Using the experimental setup, we collected 10,000 scattered images, which were randomly divided into 9,700 training samples and 300 test samples. The training samples were used for deep learning training, while the test samples were used to validate the training results of the deep learning model. We trained the deep learning model for 400 epochs, where one epoch indicates that each training sample has passed through the neural network once. After the training is complete, we can obtain the reconstructed image by simply using the generator to reconstruct the speckle image. The reconstruction results are shown in Fig. 2. "Ground Truth" refers to the original image, while "Speckle Pattern" denotes the speckle image captured by the CCD after the laser light carrying the original image information is transmitted through the optical fiber. "Reconstruction" represents the image reconstructed by inputting the scattered image into the generator after the deep learning training is completed. We evaluate the similarity of the reconstructed image with the original image using the Structural Similarity Index (SSIM), which ranges from -1 to 1. A value of 1 indicates that the two images are identical, 0 indicates no similarity, and negative values indicate significant differences in image structure. The average SSIM obtained from this reconstruction was 0.56, with a maximum SSIM of 0.78.

4. Conclusions

In this paper, we use the Pix2Pix GAN to reconstruct images transmitted through optical fibers. We demonstrate that deep learning can effectively reconstruct speckle images; however, there is still significant room for improvement. This includes designing more complex neural networks to enhance reconstruction quality and considering various polarization angles and optical fiber specifications.

REFERENCES

- [1] J. P. Dumas, M. A. Lodhi, B. A. Taki, W. U. Bajwa, and M. C. Pierce, "Computational endoscopy—a framework for improving spatial resolution in fiber bundle imaging," *Opt. Lett.*, vol. 44, no. 16, pp. 3968-3971, **2019**.
- [2] B. Rahmani, I. Oguz, U. Tegin, J.-L. Hsieh, D. Psaltis, and C. Moser, "Learning to image and compute with multimode optical fibers," *Nanophotonics*, vol. 11, no. 6, pp. 1071-1082, Mar. **2022**.
- [3] Y. Choi, C. Yoon, M. Kim, T. D. Yang, C. Fang-Yen, R. R. Dasari, K. J. Lee, and W. Choi, "Scanner-free and wide-field endoscopic imaging by using a single multimode optical fiber," *Phys. Rev. Lett.*, vol. 109, no. 20, Nov. **2012**, Art. no. 203901.
- [4] L. Wan, Z. Chen, H. Huang, and J. Pu, "Focusing light into desired patterns through turbid media by feedback-based wavefront shaping," *Appl. Phys. B, Lasers Opt.*, vol. 122, no. 7, pp. 1-7, Jul. **2016**.
- [5] A. Gover, C. Lee, and A. Yariv, "Direct transmission of pictorial information in multimode optical fibers," *JOSA*, vol. 66, no. 4, pp. 306-311, **1976**.
- [6] X. Lai, Q. Li, X. Wu, G. Liu, Z. Chen, and J. Pu, "Mutual transfer learning of reconstructing images through a multimode fiber or a scattering medium," *IEEE Access*, vol. 9, pp. 68387-68395, **2021**.
- [7] Y. Li, Y. Xue, and L. Tian, "Deep speckle correlation: A deep learning approach toward scalable imaging through scattering media," *Optica*, vol. 5, no. 10, pp. 1181-1190, **2018**.
- [8] P. Isola, et al, "Image-to-image translation with conditional adversarial networks," *IEEE Conference on Computer Vision and Pattern Recognition (CVPR)*, pp. 5967-5976, **2017**.

No. P-6

TITLE: *Ab initio* Studies of Work Function Changes of NO Combined with NO₂, CO, CO₂, H₂S, and O₃ Co-Adsorption on ZnGa₂O₄(111) Surface for Gas Sensors

Guan-Yu Chen^{†,1} and Po-Liang Liu^{*,1,2}

¹ Graduate Institute of Precision Engineering, National Chung Hsing University, Taichung 40227, Taiwan

² Department of Applied Materials and Optoelectronic Engineering, National Chi Nan University, Nantou 54561, Taiwan

[†]Presenter

*Corresponding author's e-mail: pliu@dragon.nchu.edu.tw

ABSTRACT

This study employs first-principles calculations based on density functional theory to investigate the effects of combined adsorption of NO with other gases, such as nitrogen dioxide (NO₂), carbon monoxide (CO), carbon dioxide (CO₂), hydrogen sulfide (H₂S), and ozone (O₃), on the work function changes of the clean ZnGa₂O₄(111) surface. The results indicate that the adsorption of pure NO on the clean ZnGa₂O₄(111) surface leads to a work function change of 0.32 eV, demonstrating a significant impact of NO adsorption on the electronic properties of the surface. When NO is adsorbed in combination with H₂S, the highest work function change among all gas combinations reaches 1.24 eV, suggesting that the synergistic effect of NO and H₂S significantly enhances the alterations in the surface electronic structure, which could have important implications for gas sensor performance. These findings not only advance our understanding of the interactions between the ZnGa₂O₄(111) surface and various gas combinations, but also provide a solid theoretical foundation for the design of more efficient gas sensors, particularly for detecting NO in conjunction with H₂S and other gases.

Keywords: First-principles; ZnGa₂O₄ epilayer; Gas sensor; Nitric oxide; Nitrogen Dioxide; Carbon Monoxide; Carbon Dioxide; Hydrogen Sulfide; Ozone; Work function changes; Density functional theory; Co-adsorption

REFERENCES

- [1] Bruckdorfer, R. The basics about nitric oxide. *Molecular Aspects of Medicine* 26, 3-31 (2005).
- [2] Jain, G.H. MOS gas sensors: What determines our choice. *5th Int Conf Sens Technol* 66-72 (2011).
- [3] Li, L., Hsu, A. & Moore, P.K. Actions and interactions of nitric oxide, carbon monoxide and hydrogen sulphide in the cardiovascular system and in inflammation — a tale of three gases. *Pharmacol Ther* 123, 386-400 (2009).
- [4] Jia, C., Fan, W., Yang, F., Zhao, X., Sun, H., Li, P. & Liu, L. A theoretical study of water adsorption and decomposition on low-index spinel ZnGa₂O₄ surfaces: correlation between surface structure and photocatalytic properties. *ACS* 29, 7025-7037 (2013).
- [5] Hafner, J. *Ab initio* simulations of materials using VASP: Density-functional theory and beyond. *Journal of Computational Chemistry* 29, 2044-2078 (2008).

No. P-7

TITLE: Enhanced Performance of MOCVD grown Zn-doped β -Ga₂O₃ Deep-Ultraviolet Photodetectors on Si Substrates via TiN Buffer Layers

Tung-Han Wu^{†,1}, Wen-Hao Li², Anoop Kumar Singh^{2,3}, Jun-Hong Shen¹, Shiming Huang^{2,3}, Wei-Hsiang Chiang², Hsin-Yu Chou², Po-Liang Liu^{#,1,3}, Ray-Hua Horng⁴, and Dong-Sing Wu^{*,2,3}

¹ Graduate Institute of Precision Engineering, National Chung Hsing University, Taichung 40227, Taiwan

² Department of Materials Science and Engineering, National Chung Hsing University, Taichung 40227, Taiwan

³ Department of Applied Materials and Optoelectronic Engineering, National Chi Nan University, Nantou 54561, Taiwan

⁴ Institute of Electronics, National Yang Ming Chiao Tung University, Hsinchu 30010, Taiwan

[†]Presenter

*Corresponding author's e-mail: dsw@ncnu.edu.tw #Corresponding author's e-mail: pliu@dragon.nchu.edu.tw

ABSTRACT

β -Ga₂O₃ is renowned as an emerging semiconductor material due to its wide bandgap (4.2-4.9 eV) and high electrical breakdown field (8 MV/cm) [1,2]. However, it faces significant challenges on silicon substrates due to lattice and thermal expansion mismatches, which can lead to defects that degrade performance. Therefore, this work explores the utilization of a titanium nitride (TiN) buffer layer in order to enhance the performance of MOCVD grown Zn-doped β -Ga₂O₃-based deep-ultraviolet (DUV) photodetectors (PDs) on silicon substrates with 12, 24, and 36 sccm diethylzinc (DEZn) flow rates. The 12 sccm Zn-doped β -Ga₂O₃/TiN/Si PDs demonstrated an exceptional maximum responsivity of 31.4 A/W, which is 7 times higher compared to the undoped β -Ga₂O₃/TiN/Si (4.47 A/W) under a 5 V bias and 240 nm wavelength illumination. This PD possess quick rise time of 6.5 s and fall time of 0.5 s. This work demonstrates that TiN buffer layers and Zn doping significantly improve the performance and reliability of β -Ga₂O₃-based DUV photodetectors on silicon substrates.

Keyword: Zn-doped β -Ga₂O₃; Deep-ultraviolet photodetectors; Silicon; TiN buffer layer

REFERENCES

- [1] T. Zhang, Z. Hu, Y. Li, Q. Cheng, J. Ma, X. Tian, C. Zhao, Y. Zuo, Q. Feng, Y. Zhang, J. Ning, H. Zhou, C. Zhang, J. Zhang, Y. Hao, Influence of Oxygen on β -Ga₂O₃ Films Deposited on Sapphire Substrates by MOCVD, ECS J. Solid State Sci. Technol. 10 (2021) 075009.
- [2] R.H Horng, D.S. Wu, P. L.Liu, A. Sood, F. G.Tarntair, Y.H. Chen, J.P.Singh, and C.L.Hsiao, "Growth mechanism and characteristics of β -Ga₂O₃ heteroepitaxially grown on sapphire by metalorganic chemical vapor deposition." Materials today Advances, Vol. 16 pp. 100320 (2022).

No. P-8

TITLE: Effects of progressive energy and single energy on the electrical performance of Ar ion-implantation AlGaInP Micro-LEDs

Shiang-Jiun Lo^{†,1}, Yu-Chih Hsu¹, Yen-Ru Chen¹, Wei-Hsiang Chiang², Po-Liang Liu^{#,1,3} and Dong-Sing Wu^{*,2,3}

¹ Graduate Institute of Precision Engineering, Nation Chung Hsing University, Taichung, Taiwan

² Department of Materials Science and Engineering, Nation Chung Hsing University, Taichung, Taiwan

³ Department of Applied Materials and Optoelectronic Engineering, National Chi Nan University, Nantou, Taiwan

[†]Presenter

[#]Corresponding author's e-mail: pliu@dragon.nchu.edu.tw *Corresponding author's e-mail: dsw@ncnu.edu.tw

ABSTRACT

This study investigates advancements in the manufacturing process of AlGaInP-based Micro-LEDs, emphasizing the transition from conventional dry etching techniques to ion implantation for improved precision and device performance. Traditionally, dry etching has played a critical role in LED fabrication due to its effectiveness in pattern definition and material removal [1]. However, its intrinsic characteristics, including surface roughness and microstructural damage, often lead to the need for post-etch repair and planarization [2]. Ion implantation, a non-contact technique, offers precise control over ion depth and distribution, which can modify electronic and optical properties without compromising the epitaxial layer. This method bypasses additional physical and chemical damages and obviates the need for surface planarization [3]. While ion implantation technology has shown significant success in enhancing the performance of blue Micro-LEDs [4-5], its application in red-emitting LEDs remains underexplored. This research therefore focuses on evaluating the electrical characteristics of AlGaInP Micro-LEDs, specifically contrasting the outcomes of progressive multi-energy ion implantation versus single-energy Ar ion implantation. Utilizing SRIM simulations, the study examines the impact of both implantation strategies on insulation, leakage current, turn-on voltage, and I-V curve. The findings reveal that progressive multi-energy ion implantation significantly improves internal insulation compared to single-energy implantation. For instance, under a reverse bias of 5 V, the leakage current in single-energy devices registers at 10^{-6} A, whereas progressive energy implantation reduces this to 10^{-8} A two-order magnitude reduction. This improvement is attributed to the more uniform defect distribution created by progressive implantation, effectively minimizing carrier scattering and lowering leakage current. Furthermore, at a forward bias of 5 V, progressive implantation achieves a current of 12.92 mA, a 21.9% increase compared to the 10.6 mA seen in single-energy implantation. Additionally, at an injection current of 1 mA, the turn-on voltage drops from 3.22 V to 2.55 V, reflecting a 20.8% decrease. These results underscore how progressive ion implantation enhances drive efficiency by lowering the turn-on voltage in Micro-LED devices. In summary, this study provides critical insights into how varying ion implantation energies influence Micro-LED device characteristics, with evidence supporting the superior insulation and reduced turn-on voltage achieved through progressive multi-energy implantation. This work contributes to the foundational knowledge required to further optimize Micro-LED technology for a wide range of applications.

Keywords: Ion Implantation; I-V Curve; Leakage Current; Micro-LEDs; AlGaInP; SRIM

REFERENCES

- [1] Zhao, Y., Liang, J., Zeng, Q., Li, Y., Li, P., Fan, K., ... & Wang, W. (2021). 2000 PPI silicon-based AlGaInP red micro-LED arrays fabricated via wafer bonding and epilayer lift-off. *Optics Express*, 29(13), 20217-20228.
- [2] Yang, F., Xu, Y., Li, L., Cai, X., Li, J., Tao, J., ... & Xu, K. (2022). Optical and microstructural characterization of Micro-LED with sidewall treatment. *Journal of Physics D: Applied Physics*, 55(43), 435103.

- [3] Horng, R. H., Chien, H. Y., Tarntair, F. G., & Wu, D. S. (2018). Fabrication and study on red light micro -LED displays. *IEEE Journal of the Electron Devices Society*, 6, 1064-1069.
- [4] Hsu, Y. H., Wang, C. H., Lin, X. D., Lin, Y. H., Wu, D. S., & Horng, R. H. (2023). Improved electrical properties of micro light-emitting diode displays by ion implantation technology. *Discover Nano*, 18(1), 48.
- [5] Ye, J., Peng, Y., Luo, C., Wang, H., Zhou, X., Guo, T., ... & Wu, C. (2023). Pixelation of GaN based Micro-LED arrays by tailoring injection energy and dose of fluorine ion implantation. *Journal of Luminescence*, 261, 119903.

No. P-9

TITLE: Investigation of Smart Fan

Hsinn-Jyh Tzeng* and jia-hao Huang†

Department of Mechanical Engineering, Southern Taiwan University of Science and Technology, Taiwan

†Presenter

*Corresponding author's e-mail: hjtzeng@stust.edu.tw

ABSTRACT

This study explores the smart fan is utilized temperature and humidity sensors to adjust automatically the wind speed, and providing an intelligent and comfortable user experience. It ensures the indoor temperature is regulated, allowing the fan to adapt in real-time, resulting in more efficient energy use. This enables the smart fan not only to ensure personal comfort, but also offer environmental and energy-saving benefits. In summer, air conditioning should be used in conjunction with fans for optimal efficiency. Given the global warming issue, energy-saving method was crucial, and one way to achieve this is by reducing power consumption. With inverter air conditioner already being widely used, so we drew inspiration from this concept, and developed the idea of a smart fan as the motivation for this research. Currently, global warming is indeed a significant issue that we cannot ignore. If everyone could contribute a small effort to conserve energy, it would become a tremendous force. The ultimate goal is to slow down global warming by using air conditioning less and reducing carbon emissions through energy conservation. Through experimental testing, it is really possible to achieve results in adjusting wind speed and cooling energy efficiency.

Keyword: Humidity; Intelligent; Energy-saving

REFERENCES

- [1] Iwona Grobelna, Intelligent Industrial Process Control Systems, **2023**.
- [2] Chen Sutong, Hou Chengyi, Li Yaogang, Zhang Qinghong ,Li Kerui, Wang Hongzhi, "Development Progress and Status of Smart Glasses", C.I.C.:TS959, China, **2021**, Vol.49, No.7.
- [3] Gordon D Logan, Automatic control: How experts act without thinking, **2018**.
- [4] O., & Oladunmoye a., Design and Construction of an Automatic Sliding Door Using Infrared Sensor, **2014**.
- [5] Tang Yijun, He Jianyou, Zhou Sicheng, "A Study of Global Photochromic Spectacle Lens Technology Development Trend Based on Patent Analysis", Science and Technology Innovation Herald, C.I.S.:TS959, China, No.6, **2012**, pp. 97-99.
- [6] W. kuang, L. Chen, Z. Xian, Y. Chen, "CAD/CAM/CAE Integrated Technology for out shell of Digital Camera", *Procedia Eng.*, **2011**, Volume 15, pp. 4352-4356.
- [7] Yanwei, Huyong, "Processing Parameter Optimization for Injection Moulding Products in Agricultural Equipment Based on Orthogonal Experiments and Analysis", *International Conference on Computer Distributed Control and Intelligent Environmental Monitoring*, **2011**, pp. 560-564.
- [8] N., Fangxing li, & Pei zhang, Next-Generation Monitoring, Analysis, and Control for the Future Smart Control Center, **2010**.
- [9] Babur Ozcelik, Ibrahim Sonat "Warping and structural analysis of thin shell plastic in the plastic injection molding", *Journal of Materials and Design*, **2009**, Volume 30, pp.367-375.
- [10] b. mizaikoff, S. kim C. young, *Miniaturized Mid-Infrared Sensor Technologies*, **2007**.

No. P-10

TITLE: Application of MnCsPb(Br_{0.4}/I_{0.6})₃ perovskite quantum dots in sensitized solar cells

Feng-Yuan Hsu^{†,1}, Min-Han Chiang¹, Wei-Hsiang Chiang¹, Hsin-Yu Chou¹ and Dong-Sing Wu^{*,1,2}

¹ Department of Materials Science and Engineering, Nation Chung Hsing University, Taichung, Taiwan

² Department of Applied Materials and Optoelectronic Engineering, National Chi Nan University, Nantou, Taiwan

[†]Presenter

*Corresponding author's e-mail: dsw@ncnu.edu.tw

ABSTRACT

In recent years, quantum dots have become a highly regarded research area in materials science. Early developments focused on cadmium quantum dots, which were extensively studied due to their stability and excellent photoluminescence. However, with technological advancements and increasing environmental awareness, toxic cadmium quantum dots are gradually being replaced by non-toxic perovskite quantum dots [1-2]. Perovskite quantum dots offer numerous advantages, including high quantum yield, broad absorption range, non-toxicity, and tunable luminescent properties. Consequently, they have significant application potential in solar cells, light-emitting diodes, photodetectors, and bioimaging. Nevertheless, perovskite quantum dots exhibit inferior longevity compared to cadmium quantum dots, and their emission wavelength can change as they degrade. Therefore, surface modification is necessary to prevent degradation and decline in performance before utilizing perovskite quantum dots [3]. Due to their exceptional light absorption capability and high photovoltaic conversion efficiency, perovskite quantum dots hold great potential for application in solar cells. Compared to traditional silicon-based photovoltaic materials, the bandgap of perovskite quantum dots can be precisely controlled by adjusting their composition and size, which allows for higher light absorption efficiency across the entire spectrum. However, stability issues of perovskite materials during application remain a significant challenge. These materials are prone to degradation due to environmental factors such as humidity, oxygen, and light exposure, which greatly limits their lifespan and performance in practical applications. Therefore, enhancing the stability of MnCsPb(Br_{0.4}/I_{0.6})₃ quantum dots through process optimization and material modification has become one of the main motivations for this research [4-5]. In addition to optimizing the fabrication techniques, the practical application of MnCsPb(Br_{0.4}/I_{0.6})₃ quantum dots in actual devices is also an important aspect of this study. By using process-optimized MnCsPb(Br_{0.4}/I_{0.6})₃ quantum dots to replace the active layer in traditional dye-sensitized solar cells [6], measurements taken after exposure to 365 nm UV light and sunlight showed the generation of potential difference and current. This confirms that MnCsPb(Br_{0.4}/I_{0.6})₃ quantum dots can serve as an alternative option for dye-sensitized solar cells [7].

Keyword: MnCsPb(Br_{0.4}/I_{0.6})₃ quantum dots; Chemical solution method; Process optimization; Surface Modification; Dye-sensitized solar cells

REFERENCES

- [1] Kim, J., Hwang, D. W., Jung, H. S., Kim, K. W., Pham, X. H., Lee, S. H., ... & Jun, B. H. (2022). High-quantum yield alloy-typed core/shell CdSeZnS/ZnS quantum dots for bio-applications. *Journal of nanobiotechnology*, 20(1), 22.
- [2] Zheng, N., Yan, J., Qian, W., Song, C., Zuo, Z., & He, C. (2021). Comparison of developmental toxicity of different surface modified CdSe/ZnS QDs in zebrafish embryos. *Journal of environmental sciences*, 100, 240-249.
- [3] Khan, J., Ullah, I., & Yuan, J. (2022). CsPbI₃ perovskite quantum dot solar cells: opportunities, progress and challenges. *Materials Advances*, 3(4), 1931-1952.
- [4] Huynh, K. A., Bae, S. R., Nguyen, T. V., Do, H. H., Heo, D. Y., Park, J., ... & Kim, S. Y. (2021). Ligand-assisted sulfide surface treatment of CsPbI₃ perovskite quantum dots to increase photoluminescence and recovery. *ACS Photonics*, 8(7), 1979-1987.

- [5] Yan, D., Shi, T., Zang, Z., Zhao, S., Du, J., & Leng, Y. (2020). Stable and low-threshold whispering-gallery-mode lasing from modified CsPbBr₃ perovskite quantum dots@ SiO₂ sphere. *Chemical Engineering Journal*, 401, 126066.
- [6] Ameta, C., Agarwal, R., Vyas, Y., & Chundawat, P. (2022). Outdoor Performance and Stability Assessment of Dye-Sensitized Solar Cells (DSSCs). *Chapters*
- [7] Im, J. H., Lee, C. R., Lee, J. W., Park, S. W., & Park, N. G. (2011). 6.5% efficient perovskite quantum-dot-sensitized solar cell. *Nanoscale*, 3(10), 4088-4093

No. P-11

TITLE: *Ab initio* Study of $\text{Bi}_2\text{O}_2\text{X}$ ($\text{X} = \text{Se}, \text{S}, \text{and Te}$)(001)/ SrTiO_3 (001) Heterostructures

Yan-Cheng Lin, Chun-Che Lee[†], and Po-Liang Liu^{*}

Graduate Institute of Precision Engineering, National Chung Hsing University, Taichung 40227, Taiwan

[†]Presenter

^{*}Corresponding author's e-mail: pliu@dragon.nchu.edu.tw

ABSTRACT

This study utilizes first-principles calculations based on density functional theory to investigate the structures of $\text{Bi}_2\text{O}_2\text{Se}$, $\text{Bi}_2\text{O}_2\text{S}$, and $\text{Bi}_2\text{O}_2\text{Te}$ thin films on SrTiO_3 substrates. The S-terminated $\text{Bi}_2\text{O}_2\text{S}$ (001) film exhibits the lowest heterojunction interface energy of -0.0426 to 0.1060 eV/Å² on a TiO_2 -terminated SrTiO_3 (001) substrate, indicating that a stable heteroepitaxial growth can occur with Bi bonding to TiO_2 . Similarly, the S-terminated $\text{Bi}_2\text{O}_2\text{S}$ (001) film shows a minimum heterojunction interface energy of -0.0417 to 0.1069 eV/Å² on a SrO-terminated SrTiO_3 (001) substrate, suggesting stability in heteroepitaxial growth with Bi bonding to SrO. Compared to $\text{Bi}_2\text{O}_2\text{Se}$ (001) and $\text{Bi}_2\text{O}_2\text{Te}$ (001), the $\text{Bi}_2\text{O}_2\text{S}$ (001) film exhibits the lowest interface energy values on both the TiO_2 -terminated and SrO-terminated SrTiO_3 (001) substrates, which aligns with experimental results [1].

Keyword: First-principles; 2D-material; Heterostructure; Interfacial energy

REFERENCES

- [1] B. Guo, Y. Guo, and L. Xu, "First-principles insight into the interfacial properties of epitaxial $\text{Bi}_2\text{O}_2\text{X}$ ($\text{X} = \text{S}, \text{Se}, \text{Te}$) on SrTiO_3 substrates," *Journal of Physics and Chemistry of Solids*, Vol. 163, pp. 110601 (2022).

No. P-12

TITLE: Flexible High Entropy Relaxor with Ultrahigh Energy Performance and Outstanding Piezo-
respond

Yu-En Pan^{†,1} and Ying-Hao Chu^{*,2}

¹ College of Semiconductor Research, National Tsing Hua University

² Department of Materials Science and Engineering, National Tsing Hua University

[†]Presenter

^{*}Corresponding author's e-mail: yhchu@mx.nthu.edu.tw

ABSTRACT

The growing demand for electronic devices has emphasized the need to reduce thermal loss and enhance energy efficiency. Relaxor ferroelectric material PMN-PT, an outstanding piezoelectric material known for its high dielectric permittivity and slim hysteresis loops, is commonly used in sensors and actuators. It is also a promising candidate for energy storage applications due to its minimal energy loss. Based on its excellent piezoelectric and energy performance, the concept of high-entropy was introduced into this system. Multiple atoms disrupt the long-range order of the material, forming a thermally stable system, thereby improving its thermal and electrical stability. In this study, a high-entropy relaxor ferroelectric, PMNTHZO ($\text{Pb}_{1.1}(\text{Mg}_{0.15}\text{Nb}_{0.3}\text{Ti}_{0.05}\text{Hf}_{0.25}\text{Zr}_{0.25})\text{O}_3$), was epitaxially grown via pulsed laser deposition on flexible mica and SrTiO_3 substrates. PMNTHZO demonstrated an energy efficiency exceeding 70% and a breakdown voltage over 70 V, corresponding to an electric field strength greater than 2.12 MV/cm, indicating its robustness for energy storage. The successful integration of PMNTHZO on flexible mica substrates also suggests potential for flexible electronics. The excellent thermal stability and mechanical flexibility of mica make it ideal for electronic applications, such as wearable sensors. Through the heating test, the results demonstrate that PMNTHZO can endure temperatures exceeding 250°C and 150°C separately on STO and mica, showing the robustness and thermal stability of PMNTHZO. The bending test results show that the polarization value decays less than 5% during bending cycle. The piezoelectric property is also confirmed by the PFM results and the relaxor-like P-E hysteresis loop, which makes it promising for piezoelectric devices, forming a sustainable braking system. Compared to conventional piezoelectric materials, PMNTHZO exhibits lower thermal consumption and longer cycle life, making it a potential candidate for advanced actuators. This work highlights the significant potential of combining high-entropy oxide compounds with ferroelectric relaxors for developing advanced, flexible, and thermally stable dielectric energy storage devices.

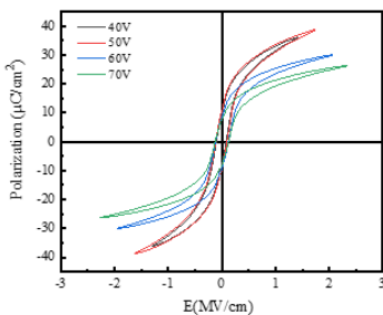


Figure 1. P-E hysteresis loop (PMNTHZO on STO substrate)

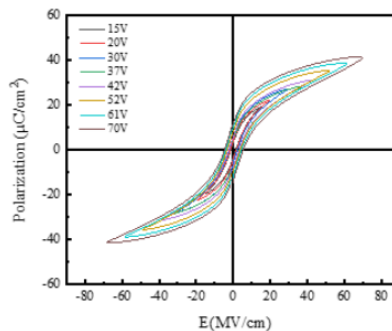


Figure 2. P-E hysteresis loop (PMNTHZO on mica substrate)

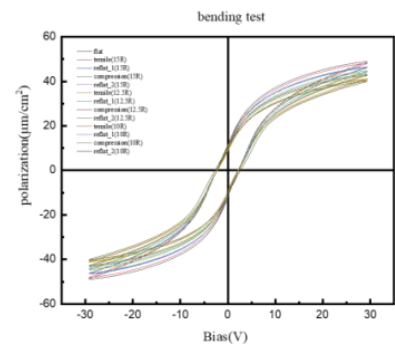


Figure 3. bending test (PMNTHZO on mica substrate)

Keyword: High entropy; Relaxor ferroelectric; Energy storage; Piezoelectric

REFERENCES

- [1] Wang, Y., Lai, H., Chen, Y., Huang, R., Hsin, T., Liu, H., Zhu, R., Gao, P., Li, C., Yu, P., Chen, Y., Li, J., Chen, Y., Yeh, J., & Chu, Y. (2023). High Entropy Nonlinear Dielectrics with Superior Thermally Stable Performance. *Advanced Materials*, 35(47).
- [2] Hao, X. (2013). A review on the dielectric materials for high energy-storage application. *Journal of Advanced Dielectrics*, 03(01), 1330001.

No. P-13

TITLE: Single-Crystalline Ag Nanocrystals Intercalated Muscovite

Chia-Yun Sung^{†,1}, Wan-Zhen Hsieh², Ching-Yu Chiang², Kuo-Ping Chen³ and Ying-Hao Chu^{*,4}

¹ Department of Materials Science and Engineering, National Yang Ming Chiao Tung University, Hsinchu City, Taiwan

² National Synchrotron Radiation Research Center (NSRRC), Hsinchu City, Taiwan

³ Institute of Photonics Technologies, Department of Electrical Engineering, National Tsing Hua University, Hsinchu City, Taiwan

⁴ Department of Materials Science and Engineering, National Tsing Hua University, Hsinchu City, Taiwan

[†]Presenter

*Corresponding author's e-mail: yhchu@mx.nthu.edu.tw

ABSTRACT

Environmental pollution has become a critical issue with the increasing global population and industrial development. Detecting water pollutants is the first step toward controlling pollution sources. This study aims to develop a SERS substrate by combining silver nanoparticles and artificial muscovite for pollutant detection. Through hydrothermal method and vacuum annealing, Ag NPs were uniformly synthesized within the muscovite layers, forming a mesocrystal system. The Ag NPs exhibited high crystallinity, with an average particle size of 82 nm and a coverage rate of 38.9%. XRD analysis confirmed an epitaxial relationship between Ag (111) and muscovite (001), while Laue diffraction revealed a well-ordered 3D mesocrystal structure. SERS with probe molecules Rhodamine 6G (R6G) and Crystal Violet (CV) demonstrated the detection limit as low as 10^{-6} M and 10^{-7} M separately. This Ag/muscovite mesocrystal system shows great potential as a highly sensitive solid substrate for environmental pollutant detection.

Keyword: Intercalation; Mesocrystal; Ag Nanocrystals; SERS

REFERENCES

- [1] Babicheva, Viktoriia E., *Nanomaterials* **2023**,13.7, 1270
- [2] Rycenga, Matthew, et al., *Chemical Reviews* **2011**, 111.6, 3669-3712.
- [3] Yen, M., Bitla, Y., and Chu, Y. H., *Materials Chemistry and Physics* **2019**, 234, 185-195.
- [4] Alcantar, Norma, Jacob Israelachvili, and Jim Boles., *Geochimica et Cosmochimica acta* **2003**, 67.7, 1289-1304.

No. P-14

TITLE: Flexible Magnetolectric Transducer Based on Muscovite Heterostructure

Ya-Jing Wu[†], Yong-Jyun Wang, and Ying-Hao Chu^{*}

Department of Materials Science and Engineering, National Tsing Hua University, Taiwan

[†]Presenter

^{*}Corresponding author's e-mail: yhchu@mx.nthu.edu.tw

ABSTRACT

Electric power is vital in modern life, and the demand for electricity keeps increasing. To address the growing gap between electricity supply and demand, it is essential to explore new methods of power issues. While ongoing efforts are to improve the electrical grid, another promising solution is the development of a transducer that can harvest energy. Soft materials and system integration are critical ideas for this flexible device. In this work, the multi-phase magnetolectric (ME) materials are composed of magnetic and piezoelectric components. Materials with magnetostriction have strain while a magnetic field is applied, and piezoelectric materials generate voltage output through lattice deformation. Additionally, it is necessary to consider the magnetolectric coupling effects and the substrate properties, as the component practicality is also crucial.

Besides improving energy conversion efficiency, the device's compatibility with its environment is also essential. Devices that can maintain regular operation in extreme conditions are beneficial for sustainable use. After extensive comparison, this study chose mica as the substrate for thin film growth. Mica has a two-dimensional layered structure with flexible mechanical properties under specific thicknesses, and it also offers transparency and high thermal and chemical stability. Functional oxide films are grown on mica substrates using van der Waals epitaxy. The lack of strong bonding between the substrate and the film prevents the clamping effect, thereby preserving the piezoelectric and magnetostriction properties. Thin film materials are spinel cobalt ferrite (CoFe_2O_4 , CFO) and perovskite lead zirconate titanate ($\text{PbZr}_{0.52}\text{Ti}_{0.48}\text{O}_3$, PZT) due to their high lattice compatibility. CFO is sensitive to external magnetic fields and has considerable electrical resistance, which is feasible for leakage current reduction. PZT performs well on piezoelectricity and high thermal sustainability due to its high Curie temperature ($\sim 390^\circ\text{C}$).

The epitaxial (PZT, CFO) heterostructure was fabricated using physical vapor deposition methods. Artificial mica was cut into $1\text{cm} \times 1\text{cm}$ as substrates. The vacuum chamber was evacuated to 5×10^{-5} Torr before deposition. A dual target was used during the deposition, and oxygen and argon were introduced into the atmosphere. The flexible ME system has been demonstrated in three architectures: epitaxial, polycrystalline, and nanostructure on mica. The CFO and PZT heterostructure is characterized by magnetostriction and piezoelectric properties. A series of analyses comprehensively demonstrated the crystal structure, crystalline quality, electrical and magnetic properties, and magnetolectric coupling.

With the well-performed material properties, the exciting application of this technology is to design electronic artificial skin capable of harvesting mechanical energy generated through exercise, such as activities performed in the gym. This artificial skin can convert the mechanical power produced by physical movement into electrical energy, creating a spontaneous harvest of energy from the body's activity. The energy-harvesting system holds great potential for wearable electronics, biomedical devices, and fitness technologies. This development opens exciting possibilities for self-powered devices, contributing to a sustainable and energy-efficient future.

Keyword: Flexible; Magnetolectric; $\text{CoFe}_2\text{O}_4/\text{Pb}(\text{Zr},\text{Ti})\text{O}_3$; Mica; Transducer

REFERENCES

- [1] Wang, Y. J., Chen, J. W., Lai, Y. H., Shao, P. W., Bitla, Y., Chen, Y. C., & Chu, Y. H. Flexible magnetoelectric complex oxide heterostructures on muscovite for proximity sensor. *npj Flexible Electronics* **2023**, 7(1), 10.
- [2] Spaldin, N. A., & Ramesh, R. Advances in magnetoelectric multiferroics. *Nature Materials* **2019**, 18(3), 203-212.

No. P-15

TITLE: Investigating the stability of microwave synthesized Pt-free catalysts for anion exchange membrane fuel cells

Yi-Jun Chen^{†,1}, Li-Hsiang Lu¹, Chih-Liang Wang^{*,1,2}, and Hsiharng Yang¹

¹ Graduate Institute of Precision Engineering, National Chung Hsing University, Taichung City 402202, Taiwan

² Department of Materials Science and Engineering, National Tsing Hua University, Hsinchu City 300044, Taiwan

[†]Presenter

*Corresponding author's e-mail: wangcl@mx.nthu.edu.tw

ABSTRACT

The microwave-assisted synthesis method offers advantages such as rapid heating, uniform reaction, and high selectivity, significantly reducing synthesis time and enhancing catalyst performance compared to traditional chemical syntheses. In this regard, the study aims to investigate the application of microwave-assisted synthesis in the development of Pt-free catalysts for anion exchange membrane fuel cells. The Pd-CeO₂/C and Ag/C were selected as the anode and cathode catalysts, respectively, and synthesized by a microwave-assisted method. The related properties of both catalysts were systemically characterized by X-ray diffraction (XRD), transmission electron microscopy (TEM), and electrochemical active surface area (ECSA). The results indicated that the Pd-CeO₂/C catalyst synthesized via the microwave-assisted method can exhibit better dispersion and stability to degradation in accelerated degradation tests, as compared to catalysts prepared by traditional synthesis methods. Additionally, the cathode catalyst of Ag/C can be also successfully synthesized by using the microwave method, which can have different influences on catalytic activity and stability as compared to different syntheses. The cathode and anode catalysts prepared by the microwave-assisted synthesis above are then assembled in the single cell to evaluate the device performance and discussed in the presentation.

Keyword: Microwave-assisted synthesis; Pt-free catalyst; Anion exchange membrane fuel cell

No. P-16

TITLE: Design And Comparison of Acceleration Feedback Control for Improving the Vibration Suppression and Motion Performance of Servomechanisms

Yu-Min Ren^{†,1} and Syh-Shiuh Yeh^{*,2}

¹ Institute of Mechatronic Engineering, NTUT, Taipei 10608, Taiwan

² Department of Mechanical Engineering, NTUT, Taipei 10608, Taiwan

[†]Presenter

^{*}Corresponding author's e-mail: ssyeh@ntut.edu.tw

ABSTRACT

Owing to rapid progress in the automation industry, servomotors with smaller sizes, lighter weights, and lower manufacturing costs are widely used in various mechatronic equipment, including computer numerical control machine tools and industrial robot arms. Generally, increasing the stiffness of the transmission system (including the transmission mechanisms and coupling devices) used to connect the servomotor and mechanical payload reduces the payload vibration. However, the manufacturing cost of the transmission system and power of the servomotor will also be high, and the cost and weight of the mechatronic equipment will increase. Nevertheless, reducing the stiffness of the transmission system may cause significant payload vibrations, which may cause operational problems in mechatronic equipment, such as reduced motion accuracy and increased payload settling time. Therefore, this study designs different feedback controllers based on the acceleration feedback control of the payload and compared the influences of different controllers on the improvement of vibration suppression and payload motion performance.

Acceleration feedback control has been under development for a long time and can be used to increase the bandwidth of control systems, improve the accuracy of servomotor motion, and suppress the vibration of mechanical payloads. Ding et al. [1] used acceleration feedback control in a fast tool servo system to address the problem of insufficient dynamic stiffness caused by large cutting depths. Tian et al. [2] applied acceleration feedback control to enhance the robustness and stability of the closed-loop control system of a fast-steering mirror system. When a two-mass mechanical system is operating, the servomotor can be affected by the payload so that the servomotor can produce vibrations, and payload motions are simultaneously affected. Thus, Helma et al. [3] applied acceleration feedback in a proportional-integral-derivative control structure to make the servomotor response faster and more stable as well as reduce payload vibrations. Tang et al. [4] used acceleration feedback control to improve the low-speed tracking accuracy of a telescope elevation system while also increasing the bandwidth of the closed-loop control system and reducing the influence of mechanical resonance. Because the external disturbance exerted on the servomotor also affects the payload response, Kai et al. [5] used acceleration feedback control to effectively mitigate the influence of external disturbances on payload motions and shorten the payload settling time. Ahmet [6] used acceleration feedback control to effectively suppress the influence of external disturbances on servomotor motion. Trung and Iwasaki [7] used H-infinity and acceleration feedback controls to design a robust control system to improve the motion performance and stability of flexible robots.

Although existing acceleration feedback control methods can effectively improve the motion performance of servomotor driven servomechanisms, the complex control structure and computational burden may limit the implementation of these control methods in compact control systems. Therefore, this study integrates the proportional-proportional-integral control that is widely used in commercial servomotor drives, the current compensation, and the payload acceleration feedback control to design acceleration proportional feedback control, acceleration proportional-integral feedback control, acceleration proportional-derivative feedback control, and acceleration proportional-integral-derivative feedback control. Then, the effects of different acceleration feedback controls on payload vibration suppression and motion performance are

discussed and compared. In addition, this study conducts a stability analysis of the acceleration feedback control systems, determines the stable ranges of the control parameters, and applies the particle swarm optimization algorithm to obtain the optimal control parameters, which can impartially compare the execution performance of each acceleration feedback control design. Although each feedback control design has a different degree of influence on the payload vibration suppression and motion performance during servomotor motions, overall, the acceleration proportional-integral-derivative feedback control design can improve vibration suppression by up to 20% and shorten settling time by up to 30%.

Industrial automation is developing rapidly. Thus, high accuracy, fast responses, and continuous stability have become the most important issues in the control of mechatronic equipment. Mechatronic equipment may generate vibrations during operation. However, if vibrations occur, they could affect both the operating performance of the mechatronic equipment and the time required for the equipment to reach a stable condition. Therefore, this study designs and discusses different payload acceleration feedback controls and uses the particle swarm optimization algorithm to optimize the control parameters, which can simultaneously suppress vibration and improve the motion performance of the payload. This study should be followed by a comparison of other vibration suppression methods, such as notch filter design and input shaping design, to evaluate the suppression effect of acceleration feedback control on different vibration modes and to confirm the applicable conditions and possible applications of acceleration feedback control.

Keyword: Acceleration feedback control; Vibration suppression; Motion performance; Servomechanisms

REFERENCES

- [1] Ding, F.; Luo, X.; Cai, Y.; Chang, W. Acceleration Feedback Control for Enhancing Dynamic Stiffness of Fast Tool Servo System Considering the Sensor Imperfections. *Mechanical Systems and Signal Processing* **2020**, 141.
- [2] Tian, J.; Yang, W.; Peng, Z.; Tang, T. Inertial Sensor-Based Multiloop Control of Fast Steering Mirror for Line of Sight Stabilization. *Optical Engineering* **2016**, 55(11).
- [3] Helma, V.; Goubaj, M.; Ježek, O. Acceleration Feedback in PID Controlled Elastic Drive Systems. *IFAC-PapersOnLine* **2018**, 214-219.
- [4] Tang, T.; Zhang, T.; Du, J.F.; Ren, G.; Tian, J. Acceleration Feedback of a Current-Following Synchronized Control Algorithm for Telescope Elevation Axis. *Research in Astronomy and Astrophysics* **2016**, 16(11).
- [5] Kai, T.; Sekiguchi, H.; Ikeda, H. Relative Vibration Suppression in a Positioning Machine Using Acceleration Feedback Control. *IEEJ Journal of Industry Applications* **2018**, 7(1), 15-21.
- [6] Ahmet, G. Modified Acceleration Feedback for Practical Disturbance Rejection in Motor Drives. *Turkish Journal of Electrical Engineering and Computer Sciences* **2018**, 26(4), 2151-2161.
- [7] Trung, T.V.; Iwasaki, M. Robust 2-DOF Controller Design Using H_∞ Synthesis for Flexible Robots. *IEEJ Journal of Industry Applications* **2019**, 8(4), 623-631.

No. P-17

TITLE: First Principles Study of Band Structures with Vertical Electric Field of $\text{Bi}_2\text{O}_2\text{S}$ and $\text{Bi}_2\text{O}_2\text{Te}$ Structures

Tzu-Wei Wang^{†,1}, Sylvia-Qingyu Cai², Chao-Cheng Kaun², and Po-Liang Liu^{*,1,3}

¹ Graduate Institute of Precision Engineering, National Chung Hsing University, Taichung 40227, Taiwan

² Research Center for Applied Sciences, Academia Sinica, Taiwan

³ Department of Applied Materials and Optoelectronic Engineering, National Chi Nan University, Nantou 54561, Taiwan

[†]Presenter

*Corresponding author's e-mail: pliu@dragon.nchu.edu.tw

ABSTRACT

The field of two-dimensional(2D) materials has been extensively studied since the method of separating single-layer graphene from graphite was discovered in 2004. The 2D layered bismuth oxychalcogenide $\text{Bi}_2\text{O}_2\text{X}$ ($X = \text{S}, \text{Se}, \text{Te}$) material has good structural stability properties and high electron mobility of $410 \text{ cm}^2/\text{V}\cdot\text{s}$ at room temperature. Bismuth oxyselenide ($\text{Bi}_2\text{O}_2\text{Se}$) is a new high-mobility semiconductor with band gap 0.8 eV . bismuth oxytelluride ($\text{Bi}_2\text{O}_2\text{Te}$) and bismuth oxysulfide ($\text{Bi}_2\text{O}_2\text{S}$) are the same. All bismuth oxychalcogenides have adjustable band gap characteristics. $\text{Bi}_2\text{O}_2\text{X}$ ($X = \text{S}, \text{Se}, \text{Te}$) materials can change the conductive band and valence of the material's band structure by changing the number of layers or applying an external electric field. Electric band closure, in order to understand the number of layers of the $\text{Bi}_2\text{O}_2\text{X}$ structure and the impact of the external electric field on the band structure, this study uses first principles calculations based on density functional theory(DFT) to evaluate the band structure changes in the 2D $\text{Bi}_2\text{O}_2\text{S}(001)$, $\text{Bi}_2\text{O}_2\text{Te}(001)$ structure, and $\text{Bi}_2\text{O}_2\text{S}(001)/\text{Bi}_2\text{O}_2\text{Te}(001)$ heterostructure under applied vertical electric fields. The analysis of band structure trends helps elucidate the effects of structure and vertical electric field on the band structures, the lattice constants and angles in the structures of $\text{Bi}_2\text{O}_2\text{S}$ and $\text{Bi}_2\text{O}_2\text{Te}$ are close to the experimental results. The lattice constants after the optimized of $\text{Bi}_2\text{O}_2\text{S}$ structure are $a = b = 3.87 \text{ \AA}$, $c = 12.10 \text{ \AA}$; The lattice constants after the optimized of $\text{Bi}_2\text{O}_2\text{Te}$ are $a = b = 4.01 \text{ \AA}$, $c = 12.70 \text{ \AA}$, $\alpha = \beta = \gamma = 90^\circ$, the space groups are all $I4/mmm$, the applied electric field directed perpendicular to the xy plane of $\text{Bi}_2\text{O}_2\text{S}(001)$, $\text{Bi}_2\text{O}_2\text{Te}(001)$ structure, and $\text{Bi}_2\text{O}_2\text{S}(001)/\text{Bi}_2\text{O}_2\text{Te}(001)$ heterostructure. The band structure of the $\text{Bi}_2\text{O}_2\text{S}(001)$ structure, without the influence of a vertical electric field, shows that the valence band crosses the fermi level without overlapping with the conduction band, thereby exhibiting semi-metallic characteristics. As the vertical electric field is applied from 0 V/\AA to 0.03 V/\AA , a gradual closure in the band structure of the $\text{Bi}_2\text{O}_2\text{S}(001)$ structure is observed. The band structure of the $\text{Bi}_2\text{O}_2\text{Te}(001)$ structure, without the influence of a vertical electric field, shows that the valence band crosses the fermi level without overlapping with the conduction band, thereby exhibiting semi-metallic characteristics. The band structure gradually closes and the valence and conduction bands overlap. Under the influence of the vertical electric field, the $\text{Bi}_2\text{O}_2\text{Te}(001)$ structure transitions from a semi-metal to a conductor, displaying metallic characteristics. The band structure of the $\text{Bi}_2\text{O}_2\text{S}(001)/\text{Bi}_2\text{O}_2\text{Te}(001)$ heterostructure, without the influence of a vertical electric field, shows that the valence band crosses the Fermi level without overlapping with the conduction band, thereby exhibiting semi-metallic characteristics. As the vertical electric field is applied from 0 V/\AA to 0.03 V/\AA , a gradual closure in the band structure of the $\text{Bi}_2\text{O}_2\text{S}(001)/\text{Bi}_2\text{O}_2\text{Te}(001)$ heterostructure is observed. This study proves that an external vertical electric field can adjust the energy band structure of the $\text{Bi}_2\text{O}_2\text{S}(001)$, $\text{Bi}_2\text{O}_2\text{Te}(001)$ structure, and $\text{Bi}_2\text{O}_2\text{S}(001)/\text{Bi}_2\text{O}_2\text{Te}(001)$ heterostructure to close as the magnitude of the applied vertical electric field increases.

Keyword: *Ab initio* calculation; Two-dimensional materials; Band structures; Vertical electric field

REFERENCES

- [1] K. S. Novoselov, A. K. Geim, S. V. Morozov, D. Jiang, Y. Zhang, S. V. Dubonos, I. V. Grigorieva, A. A. Firsov, *Science*, 306 (2004) 666-669.
- [2] Q. Wei, R. Li, C. Lin, A. Han, A. Nie, Y. Li, L. J. Li, Y. Cheng, W. Huang, *ACS Nano* 2019, 13 (2019) 13439-13444.
- [3] J. Q. Li, C. Cheng, M. Y. Duan, *Applied Surface Science*, 618 (2023) 156541.
- [4] U. Khan, R. Xu, A. Nairan, M. Han, X. Wang, L. Kong, J. Gao, L. Tang, *Advanced Functional Materials*, 34 (2024) 2315522.

No. P-18

TITLE: Integrated Microfluidic Photoresistor System for Determining Human Serum Albumin

To-Lin Chen[†], Kuan-Hsun Huang, Ching-Ti Wang, and Lung-Ming Fu^{*}

Department of Engineering Science, National Cheng Kung University, Tainan, 701, Taiwan

[†]Presenter

^{*}Corresponding author's e-mail: loufyfu@ncku.edu.tw

ABSTRACT

Chronic Kidney Disease (CKD) [1-2] is a global health concern, affecting around 13.4% of the population. In Taiwan, the prevalence is particularly high, with statistics indicating that 1 in 7 individuals are likely to develop CKD. This significant incidence places a considerable burden on healthcare systems, highlighting the need for improved detection and monitoring methods to manage the progression and outcomes of CKD more effectively. This study focuses on integrating a photoresistor-based detection system [3] to investigate serum samples for determining albumin levels.

The study employed Bromocresol Green (BCG) to react with serum, forming a complex with albumin[4]. Following this reaction, a Polymethylmethacrylate (PMMA) microfluidic chip and a micro-spectrometer were used to correlate albumin concentration and optimized experimental conditions. After constructing the calibration curve, a photoresistor-based system collected data that were associated with the micro-spectrometer readings. To validate the system's stability, 30 unknown artificial serum samples were tested, resulting in a correlation coefficient of 0.9524 and a recovery rate of 92.55%. These findings demonstrate the reliability and potential of the system.

Keyword: Microfluidic chip; Photoresistor-based system; Biosensor; Albumin

REFERENCES

- [1] Kalantar-Zadeh, K., Jafar, T. H., Nitsch, D., Neuen, B. L., & Perkovic, V. Chronic kidney disease. *The lancet* **2021**, 398, 786-802.
- [2] Charles, C., & Ferris, A. H. Chronic kidney disease. *Primary Care: Clinics in Office Practice* **2020**, 47, 585-595.
- [3] Ravula, R., & Mandal, T. K. A photoresistor-based portable digital sensor for rapid colorimetric detection of Arsenic. *Microchemical Journal* **2024**, 196, 109574.
- [4] Tseng, C. C., Ko, C. H., Lu, S. Y., Yang, C. E., Fu, L. M., & Li, C. Y. Rapid electrochemical-biosensor microchip platform for determination of microalbuminuria in CKD patients. *Analytica Chimica Acta* **2021**, 1146, 70-76.

No. P-19

TITLE: Development of a Rapid Microfluidic System for Detecting Magnesium Ion in Serum

Hsing-Meng Wang¹, Cheng-Xue Yu^{†,2}, Ching-Ti Wang², and Lung-Ming Fu^{*,2}

¹ Department of Biomechanics Engineering, National Pingtung University of Science and Technology, Pingtung 912, Taiwan

² Department of Engineering Science, National Cheng Kung University, Tainan, 701, Taiwan

[†]Presenter

*Corresponding author's e-mail: loudyfu@ncku.edu.tw

ABSTRACT

In Taiwan, acute renal failure and chronic kidney disease account for a significant 7.1% of medical resources, highlighting the importance of kidney health in the healthcare system. Imbalances in essential elements, such as magnesium, can cause harm. Magnesium ions are crucial for maintaining kidney function; low magnesium levels can exacerbate chronic kidney disease, while high levels can contribute to kidney stone formation and calcification [1,2]. This underscores the importance of regulating magnesium levels for kidney health. In this study, we present a microfluidic detection system for analyzing serum samples to determine magnesium concentration. This system aims to provide an accurate and efficient analysis of magnesium levels, essential for maintaining kidney function and overall health.

The study employs 3,5-dichloro salicylaldehyde (BCSA) [3,4] to react with serum, with magnesium enhancing fluorescence. To quantify the results, a micro-spectrometer is utilized, and a microfluidic chip made from polymethylmethacrylate (PMMA), and polyethylene terephthalate (PET) is used to analyze varying magnesium concentrations. This setup enables precise detection and analysis of magnesium levels in serum samples. The results indicate a standard curve correlation coefficient of 0.9915 and artificial serum testing has a recovery rate of 96 %, underscoring the stability and reliability of the detection system when analyzing real serum samples. This innovative method demonstrates significant potential for accurately quantifying magnesium concentrations in clinical settings.

Keyword: Microfluidic; Magnesium ion

REFERENCES

- [1] Micke, O., Vormann, J., Kraus, A., & Kisters, K. Serum magnesium: Time for a standardized and evidence-based reference range. *Magnesium research* **2021**, *34*, 84-89.
- [2] Piuri, G., Zocchi, M., Della Porta, M., Ficara, V., Manoni, M., Zuccotti, G. V., ... & Cazzola, R. Magnesium in obesity, metabolic syndrome, and type 2 diabetes. *Nutrients* **2021**, *13*, 320.
- [3] Park, S., Suh, B., & Kim, C. A chalcone-based fluorescent chemosensor for detecting Mg²⁺ and Cd²⁺. *Luminescence* **2022**, *37*, 332-339.
- [4] Men, G., Chen, C., Zhang, S., Liang, C., Wang, Y., Deng, M., ... & Jiang, S. A real-time fluorescent sensor specific to Mg²⁺: crystallographic evidence, DFT calculation and its use for quantitative determination of magnesium in drinking water. *Dalton Transactions* **2015**, *44*, 2755-2762.

No. P-20

TITLE: Research of FeCoN-MgOAc/XC-72R as cathode catalysts in Alkaline Anion Exchange Membrane Fuel Cells

Ting-Syuan Li, Chia-Hsien Ko[†], and Hsiharng Yang*

Graduate Institute of Precision Engineering, National Chung Hsing University

[†]Presenter

*Corresponding author's e-mail: hsiharng@nchu.edu.tw

ABSTRACT

This study aims to investigate the preparation method of low-cost non-precious metal cathode catalysts in alkaline anion exchange membrane fuel cells (AEMFC) and to enhance power density as the experimental objective. In the experiment, carbon black (Vulcan XC72R) was used as the carrier, and FeCoN/XC-72R was successfully prepared. Additionally, the mesoporous structure of the catalyst material was enhanced by utilizing acetic acid as an inorganic template, resulting in the successful preparation of FeCoN-MgO/XC-72R catalyst. Subsequently, FeCoN-MgOAc/XC-72R catalyst was successfully synthesized through acid washing and high-temperature pyrolysis steps. The successful preparation of the catalyst was confirmed through SEM, EDS, XRD, and CV analyses. The performance of single-cell modules was tested using an ion exchange membrane (X37-50RT), with the anode utilizing commercial platinum (Pt/C) (40 wt%) and the cathode employing self-prepared catalysts. Various proportions of catalysts and ionomers were adjusted to determine the optimal loading for power density testing. CV analysis results indicated that the optimal ratio was 80:20 under different catalyst and ionomer conditions, with the optimal loading reaching 1 mg/cm², achieving a power density of 708 mW/cm². This power density is comparable to that obtained when both the anode and cathode use commercial platinum (Pt/C), aligning with the goal of our research to develop non-precious metal catalysts and enhance the power density of AEMFC.

Keyword: Alkaline anion exchange membrane fuel cell; Non-noble metal catalyst; Inorganic template; Catalyst and ionic polymer ratio; Optimal loading capacity

REFERENCES

- [1] O. Z. Sharaf, and M. F. Orhan, "An overview of fuel cell technology: Fundamentals and applications," *Renewable & Sustainable Energy Reviews*, vol. 32, pp. 810-853, Apr, **2014**.
- [2] R. O'hayre, S.-W. Cha, W. Colella, and F. B. Prinz, *Fuel cell fundamentals: John Wiley & Sons*, **2016**.
- [3] K. A. Kurdin, V. V. Kuznetsov, V. V. Sinitsyn, E. A. Galitskaya, E. A. Filatova, C. A. Belina, and K. J. Stevenson, "Synthesis and characterization of Pt-HXMoO₃ catalysts for CO-tolerant PEMFCs," *Catalysis Today*, vol. 388, pp. 147-157, Apr, **2022**.
- [4] A. Sarapuu, E. Kibena-Poldsepp, M. Borghei, and K. Tammeveski, "Electrocatalysis of oxygen reduction on heteroatom-doped nanocarbons and transition metal-nitrogen-carbon catalysts for alkaline membrane fuel cells," *Journal of Materials Chemistry A*, vol. 6, no. 3, pp. 776-804, Jan, **2018**.
- [5] K. Kisand, A. Sarapuu, J. C. Douglin, A. Kikas, A. Treshchalov, M. Kaeerik, H. M. Piirsoo, P. Paiste, J. Aruvaeli, J. Leis, V. Kisand, A. Tamm, D. R. Dekel, and K. Tammeveski, "Templated Nitrogen-, Iron-, and Cobalt-Doped Mesoporous Nanocarbon Derived from an Alkylresorcinol Mixture for Anion-Exchange Membrane Fuel Cell Application," *Acs Catalysis*, vol. 12, no. 22, pp. 14050- 14061, Nov, **2022**.
- [6] W. R. Grove, "XXIV. On voltaic series and the combination of gases by platinum," *The London, Edinburgh, and Dublin Philosophical Magazine and Journal of Science*, vol. 14, no. 86-87, pp. 127-130, 1839/02/01, **1839**.
- [7] P. C. Okonkwo, O. O. Ige, E. Barhoumi, P. C. Uzoma, W. Emori, A. Benamor, and A. M. Abdullah, "Platinum degradation mechanisms in proton exchange membrane fuel cell (PEMFC) system: A review," *International Journal of Hydrogen Energy*, vol. 46, no. 29, pp. 15850-15865, Apr, **2021**.
- [8] S. Laribi, K. Mammam, Y. Sahli, and K. Koussa, "Air supply temperature impact on the PEMFC impedance," *Journal of Energy Storage*, vol. 17, pp. 327-335, Jun, **2018**.

No. P-21

TITLE: NiCoFe layered hydroxide anode catalyst for hydrogen production in anion exchange membrane water electrolysis

Wei-Ming Chen, Ko-Hsiang Huang[†], and Hsiharnng Yang*

Graduate Institute of Precision Engineering, National Chung Hsing University

[†]Presenter

*Corresponding author's e-mail: hsiharnng@nchu.edu.tw

ABSTRACT

This study prepared nano-flower-like NiCoFe layered double hydroxide (LDH) as an efficient anode catalyst for hydrogen production in anion exchange membrane water electrolysis (AEMWE). The NiCoFe-LDH exhibited excellent oxygen evolution reaction (OER) activity, long-term stability, and high surface area characteristics. Utilizing a low-cost non-precious metal anode catalyst through ultrasonication, the catalyst was annealed at 500°C for 6 hours with a heating rate of 10°C/min in air after ultrasonication at a frequency of 40 kHz and a power of 350 W. The gas diffusion layer GDL280 and anion exchange membrane X37-50RT were employed in the experimental setup, with NiCoFe-LDH as the anode catalyst and Pt/C as the cathode catalyst. Electrochemical and material analyses were conducted, and hydrogen production tests were performed under various optimal parameters. The influence of different variables such as KOH electrolyte concentration and optimal loading amount on electrolysis performance was investigated. It was found that electrolyte concentration significantly affected electrolysis performance, with the optimal concentration being 1.5 M KOH. Using GDL280 with a higher stiffness loaded with 2 mg/cm² of NiCoFe-LDH, efficient electrolysis cells could be fabricated at an electrolyte temperature of 25°C. Overall, the highest current density obtained at 2V voltage was 1.31 A/cm² in this experiment.

Keyword: Hydrogen production; Anion exchange membrane water electrolysis; Non-noble metal catalyst; Nanopetals; High specific surface area

REFERENCES

- [1] C. Li, and J.-B. J. N. E. Baek, "The promise of hydrogen production from alkaline anion exchange membrane electrolyzers," vol. 87, pp. 106162, **2021**.
- [2] S. S. Kumar, and V. J. M. S. f. E. T. Himabindu, "Hydrogen production by PEM water electrolysis—A review," vol. 2, no. 3, pp. 442-454, **2019**.
- [3] S. Chu, and A. J. n. Majumdar, "Opportunities and challenges for a sustainable energy future," vol. 488, no. 7411, pp. 294-303, **2012**.
- [4] V. Khare, S. Nema, P. J. R. Baredar, and S. E. Reviews, "Solar–wind hybrid renewable energy system: A review," vol. 58, pp. 23-33, **2016**.
- [5] S. R. Foit, I. C. Vinke, L. G. de Haart, and R. A. J. A. C. I. E. Eichel, "Power-to-Syngas: An Enabling Technology for the Transition of the Energy System?," vol. 56, no. 20, pp. 5402-5411, **2017**.
- [6] G. W. Crabtree, and M. S. J. M. B. Dresselhaus, "The hydrogen fuel alternative," vol. 33, no. 4, pp. 421-428, **2008**.
- [7] A. Y. Faid, A. Oyarce Barnett, F. Seland, and S. J. C. Sunde, "Highly active nickel-based catalyst for hydrogen evolution in anion exchange membrane electrolysis," vol. 8, no. 12, pp. 614, **2018**.
- [8] R. Kötzt, H. Lewerenz, and S. J. J. o. T. E. S. Stucki, "XPS studies of oxygen evolution on Ru and RuO₂ anodes," vol. 130, no. 4, pp. 825, **1983**.
- [9] R. Kötzt, H. Neff, and S. J. J. o. t. E. S. Stucki, "Anodic Iridium Oxide Films: XPS-Studies of Oxidation State Changes and," vol. 131, no. 1, pp. 72, **1984**.
- [10] R. Frydendal, E. A. Paoli, B. P. Knudsen, B. Wickman, P. Malacrida, I. E. Stephens, and I. J. C. Chorkendorff, "Benchmarking the stability of oxygen evolution reaction catalysts: the importance of monitoring mass losses," vol. 1, no. 12, pp. 2075-2081, **2014**.

No. P-22

TITLE: Highly Stable ITO-based Heater With Interdigitated Electrodes

Nan-Ming Lin^{†,1}, Shih-Chang Shei², Zhi-Hong Yu³, and Shu-Wen Yang⁴

¹ N. M. Lin is with the Stanch Stainless Steel Co. Ltd, Taichung City 43509, Taiwan.

² S. C. Shei is with the Department of Electrical Engineering, National University of Tainan, Tainan 700, Taiwan.

³ Z. H. Yu is with the Department of Electrical Engineering, National University of Tainan, Tainan 700, Taiwan.

⁴ S. W. Yang is with Plan Management Section, Metal Industries Research & Development Centre, Kaohsiung 81160, Taiwan.

[†]Presenter

*Corresponding author's e-mail: nanming0520@gmail.com

ABSTRACT

The interdigitated electrodes on the conventional ITO heater (i.e. sample 2) and conventional ITO heater (i.e. sample 1) were successfully fabricated. It was found that maximum temperatures for sample 1 and sample 2 were 69 and 102 °C at 100s, respectively. The temperature of sample 2 was about 47% larger than that of sample 1. Such a significant enhancement in temperature can be attributed to the interdigitated electrodes on the top of the ITO film. Under the same 20V voltage operation, it was found that the currents for sample 1 and sample 2 were 0.13 and 0.29A, respectively. It was also calculated that the resistances for sample 1 and sample 2 were 153.8 and 68.9 Ω, respectively. It should be noted that the maximum power consumption of sample 2 was 5.8W. The larger 20V output current observed from sample 2 can again be attributed to the low resistance. Such a result indicates that the large power generation will result in the large heat generation. For the switching cycle of sample 2 between 0 and 20V for 6 cycles, it was found that the high temperature and low temperature of sample 2 was from 30 to 102°C, respectively. Such a result suggests that the ITO heater with the interdigitated electrodes can achieve good thermal stability without degradation.

Keyword: Interdigitated electrodes; Indium-tin-oxide (ITO); Heater

REFERENCES

- [1] C. Kim, J. W. Park, J. Kim, S. J. Hong, and M. J. Lee, "A highly efficient indium tin oxide nanoparticles (ITO-NPs) transparent heater based on solution-process optimized with oxygen vacancy control, *J. Alloys Compd.*, " vol.726, pp. 712-719, Dec. **2017**.
- [2] S. Bok, H. J. Seok, Y. A. Kim, J. H. Park, J. Kim, J. Kang, H. K. Kim, and B. Lim, "Transparent molecular adhesive enabling mechanically stable ITO thin films," *ACS Appl. Mater. Interfaces*, vol.13, pp. 3463-3470, Jan. **2021**.
- [3] K. Im, K. Cho, J. Kim, and S. Kim, "Transparent heaters based on solution-processed indium tin oxide nanoparticles," *Thin solid films*, vol. 518, pp. 3960-3963, May **2010**.
- [4] K. Im, K. Cho, K. Kim, K. Kwak, J. Kim, and S. Kim, "Flexible transparent heaters with heating films made of Indium tin oxide nanoparticles," *J. Nanosci. Nanotechnol.*, vol.13, pp. 3519-3521, May **2013**.
- [5] R. Pawlak and M. Lebioda, "Electrical and thermal properties of heater-sensor microsystems patterned in TCO films for wide-range temperature applications from 15 K to 350 K," *Sensors*, vol. 18, Jun. **2018**.
- [6] S. J. Hong, S. J. Cha, J. Y. Lee, and Y.S. Kim, "Improvement of particle size of indium tin oxide nanoparticles by in-situ dispersion method for solution based transparent heater," *Electron. Mater. Lett.*, vol.13 pp.37-44, Dec. **2017**.
- [7] R. Liang, H. Wang, S. Zhan, M. Y. Longlong, S. L. Fei, D. Wang, and R. Zheng, "High-temperature flexible transparent heater for rapid thermal annealing of thin films," *Phys. Rev. Applied.*, vol. 17, April **2022**, Art. no. 04409.
- [8] J. Kim, S. Kim, S. Yoon, and P. Song, "Characteristics of ITO/Ag/ITO hybrid layers prepared by magnetron sputtering for transparent film heaters," *J. Opt. Soc. Korea*, vol. 20, pp. 807-812, Dec. **2016**.
- [9] Y. C. Lin, S. J. Chang, Y. K. Su, C. S. Chang, S. C. Shei, J. C. Ke, H. M. Lo, S. C. Chen, and C. W. Kuo, "High power nitride based light emitting diodes with Ni/ITO p-type contacts," *Solid State Electron.*, vol. 47, pp. 1565-1568, sept.**2003**.
- [10] C. S. Chang, S. J. Chang, Y. K. Su, W. S. Chen, C. F. Shen, S. C. Shei, and H. M. Lo, "Nitride based power chip with indium-tin-oxide p-contact and Al back-side reflector," *J. Appl. Phys.*, vol. 44, pp. 2462-2464, Apr. **2005**.
- [11] M. Genç, V. Sheremet, M. Elçic, A. E. Kasapoğlu, İ. Altuntaş, İ. Demir, G. Eğin, S. İslamoğlu, E. Gür, N. Muzafferoğlu, S. Elagöz, O. Gülseren, and A. Aydınli, "Distributed contact flip chip InGaN/GaN blue LED; comparison with conventional LEDs," *Superlattices Microstruct.*, vol.128, pp. 9-13, Apr. **2019**.

- [12] Q. Chen, J. Dai, X. Li, Y. Gao, H. Long, Z. H. Zhang, C. Chen, and H. C. Kuo, "Enhanced Optical Performance of AlGaN-Based Deep Ultraviolet Light-Emitting Diodes by Electrode Patterns Design," *IEEE Electron Device Lett.*, vol.40, pp. 1925-1928, Dec. **2022**.
- [13] V. Sheremet, M. Genç, N. Gheshlaghi, M. Elçi, N. Sheremet, A. Aydınli, I. Altuntaş, K. Ding, V. Avrutin, Ü. Özgür, and H. Morkoç, "Two-step passivation for enhanced InGaN/GaN light emitting diodes with step graded electron injectors, " *Superlattices Microstruct.*, vol. 113, pp. 623-634, Jan. **2018**.
- [14] R. Macaluso, G. Lullo, I. Crupi, F. Caruso, E. Feltin, and M. Mosca, "Current spreading length and injection efficiency in ZnO/GaN-Based light-emitting diodes," *IEEE Tran. Electron Devices*, vol. 66, pp. 4811-4816, Oct. **2019**.
- [15] Y. S. Ting, C. C. Chen, J. K. Sheu, G. C. Chi, and J. T. Hsu, "Electrical-efficiency analysis of GaN-based light-emitting diodes with interdigitated-mesa geometry," *J. Electron. Mater.*, vol.32, pp. 312-315, May **2003**.
- [16] P. Wang, W. Wei, B. Cao., Z. Gan, and S. Liu, "Simulation of current spreading for GaN-based light-emitting diodes," *Opt. Laser Technol.*, vol. 42, pp.737-740, Jul. **2010**.
- [17] J. Ding, L. Che, X. Chen, T. Zhang, Y. Huang, Z. Huang, and Z. Zen, "Interdigital structure enhanced the current spreading and light output power of GaN-based light emitting diodes, " *IEEE Access*, vol.8, pp. 105972-105979, Jun. **2020**.
- [18] S. Huang, H. Wu, B. Fan, B. Zhang, and G. Wang, "A chip-level electrothermal-coupled design model for high-power light-emitting diodes, " *J. Appl. Phys.*, vo. 107, Mar. **2010**. Art. no. 054509.
- [19] R. H. Horng, Y. A. Lu, and D. S. Wu, "Light Extraction Study on thin-film GaN light-emitting diodes with Electrodes covering by wafer bonding and textured surfaces," *IEEE Tran. Electron Devices*, vol.57, pp. 2651-2654, Aug. **2010**.
- [20] V. Sheremet, M. Genç, M. Elçi, N. Sheremet, A. Aydınli, I. Altuntaş, K. Ding, V. Avrutin, Ü. Özgü, and H. Morkoç, "The role of ITO resistivity on current spreading and leakage in InGaN/GaN light emitting diodes," *Superlattices Microstruct.*, vol.111, pp. 1177-1194, Nov. **2017**.

No. P-23

TITLE: Electronic, and magnetic properties of the 3d transition metals substitution positions in ZnX₂O₄ (X=Al, Ga) spinel oxide: a GGA+U study

Jen-Chuan Tung^{†,1} and Po-Liang Liu^{*,2,3}

¹ Center for General Education, Chang Gung University, Taoyuan 33302, Taiwan

² Graduate Institute of Precision Engineering, National Chung Hsing University, Taichung 402, Taiwan

³ Department of Applied Materials and Optoelectronic Engineering, National Chi Nan University, Nantou 54561, Taiwan

[†]Presenter

*Corresponding author's e-mail: pliu@dragon.nchu.edu.tw

ABSTRACT

In the present theoretical study, we apply the first-principles method to study the effect of 3d transition metals (TMs), V, Cr, Mn, Fe, Co, Ni doping on the electronic and magnetic properties of ZnAl₂O₄, and ZnGa₂O₄ spinel oxide. We calculate the electronic band structures for different 3d TMs substitution sites, named as A, B, and AB sites within the generalized gradient approximation (GGA) as implemented in the Quantum Espresso package. Our calculated lattice constant for the ZnAl₂O₄ with and without GGA+U is 8.17 and 8.09 angstrom. We found that in the GGA+U scheme, the calculated lattice constant is in good agreement with experimental lattice constants of 8.09[1] angstrom. The U value for the Zn-3d, O-2p orbitals is 5.5 eV. Further, our calculated lattice constant for the ZnGa₂O₄ with and without GGA+U is 8.45 and 8.36 angstrom. Whereas the experimental lattice constant for the ZnGa₂O₄ is 8.34[2] angstrom. We found that applying the on-site U parameters not only obtaining the better lattice constants but theoretical bandgaps. Furthermore, we also study the substitution position effects of the ZnX₂O₄ spinel oxides. In the ZnX₂O₄ spinel, Zn atom is sited in the tetrahedral, A, site and the X atom is sited in the octahedral, B, site. Very interesting, if one, or both, of the tetrahedral or octahedral site is substituted by the 3d TMs. We found that these ZnX₂O₄ spinel may become half-Metal which has 100% spin polarization.

Keyword: First-principle; ZnAl₂O₄; ZnGa₂O₄

REFERENCES

- [1] Levy D.; Pavese A.; Sani A.; Pischedda V.; **2001** *Phys. Chem. Minerals* 28 612.
- [2] Josties M.; O'Neill H. S. C.; Bente K.; Brey G.; **1995** *Neues Jahrb. Mineral., Monatsh.* 6 273.

ISPE 2024

The 5th International Symposium on Precision Engineering

Nov. 8-10, 2024



ISPE 2024 Website

ORGANIZERS



CO-ORGANIZERS



SPONSORS

